*Submitted to Inorganic Chemistry*

# Synthesis and reactivity of NHC-based rhodium macrocycles

Rhiann E. Andrew and Adrian B. Chaplin*

*Department of Chemistry, University of Warwick, Gibbet Hill Road, Coventry CV4 7AL, UK.*

E-mail: a.b.chaplin@warwick.ac.uk

**Abstract**

Using a general synthetic procedure employing readily accessed terminal alkene functionalised pro-ligands and macrocyclisation by ring-closing olefin metathesis, rhodium carbonyl complexes have been prepared that contain lutidine- (**1a**; n = 1) and pyridine- (**1b**; n = 0) derived tridentate CNC macrocycles with dodecamethylene spacers. In solution **1a** shows temperature invariant time averaged $C_2$ symmetry by $^1$H NMR spectroscopy ($CD_2Cl_2$, 500 MHz), while in the solid-state two polymorphs can be obtained showing different conformations of the alkyl spacer about the metal-carbonyl bond (asymmetric and symmetric). In contrast, time-averaged motion of alkyl spacer in **1b** can be halted by cooling below 225 K ($CD_2Cl_2$, 500 MHz) and the complex crystallises as a dimer with an interesting unsupported Rh···Rh bonding interaction (3.2758(6) Å). Oxidative addition reactions of **1a** and **1b**, using MeI and $PhICl_2$, have been studied in situ by $^1$H NMR spectroscopy, although pure Rh(III) adducts can ultimately only be isolated with the pyridine-based macrocyclic ligand. The lutidine backbone of **1a** can be deprotonated by addition of $K[N(SiMe_3)_2]$ and the resulting neutral dearomatised complex (**5**) has been fully characterised in solution, by variable temperature $^1$H NMR spectroscopy, and in the solid-state, by X-ray diffraction.

**Introduction**

Complexes bearing *mer*-tridentate "pincer" ligands continue to find diverse applications in organometallic chemistry and catalysis.[1] Pincer ligands confer thermal stability and support a broad range of metal-based reactivity: reactivity that can be tuned by variation of both the axial and equatorial donors. Phosphine based systems bearing a central aryl donor (PCP) are amongst the most widely studied, with iridium derivatives notable for their high activity as alkane dehydrogenation catalysts (e.g. **A**, Chart 1).[2] Recently lutidine-derived pincer ligands have also become prominent and can support bifunctional metal-ligand reactivity through base induced pyridine dearomatisation (e.g. leading to **B**).[3,4,5] Alongside the ever-growing interest in *N*-heterocyclic carbene (NHC) ligands, CCC and CNC pincer architectures featuring *trans*-NHC donors have been prepared and partnered with a wide variety of transition elements.[6] Palladium(II) based CCC and CNC complexes have been shown to be catalytically active in C-C coupling reactions and recently, inspired by work using PCP ligands, Chianese and co-workers have used analogous NHC-based variants in iridium-catalyzed alkane dehydrogenation reactions (e.g. **C**).[7,8]

**Chart 1**: Iridium pincer complexes

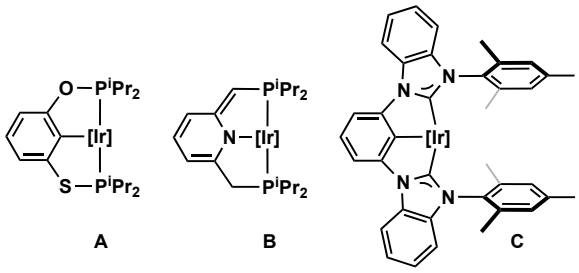


Despite facile synthetic procedures for imidazolium-based pro-ligands, the vast majority of reported CNC and CCC complexes feature NHC donors bearing simple alkyl (e.g. Me, $^{n}$Bu, $^{t}$Bu) and aryl (e.g. Mes, Dipp) appendages. Expanding on a limited number of prior examples,[9] we have recently begun exploring the coordination chemistry of macrocyclic ligands based on CNC pincer scaffolds. Our interest in this ligand topology is motived by the potential to (a) reinforce the thermal stability associated with pincer ligands through the macrocyclic effect; (b) exploit additional reaction control though their unique steric profile, especially through 'wiper-blade' like motion of the linking group; and (c) construct interlocked molecular assemblies though active-metal template strategies.[10] As part of these investigations, we have previously prepared palladium(II) derivatives of lutidine-derived CNC macrocyclic ligands containing aliphatic spacers of different length (**D**, Chart 2) and reported on how the ring size alters the structure and dynamics of the $d^8$ square planar complexes.[11] Significant ground-state steric effects are induced using the shorter spacers (m = 8, 10), while the dodecamethylene spacer (m = 12) enabled distortion-free accommodation of ancillary ligands (X = Cl, F) within the macrocycle. In this communication we expand upon the coordination chemistry of CNC macrocycles containing the latter aliphatic chain length. In particular, we describe synthetic methodology, involving olefin metathesis, that allows the preparation of NHC-based rhodium macrocycles containing both lutidine (n = 1) and pyridine (n = 0) derived CNC pincer scaffolds with

dodecamethylene spacers (**1**, Chart 2). The influence of the pincer backbone and macrocyclic topology on their dynamics and reactivity is examined.

**Chart 2**: Complexes containing CNC pincer ligands

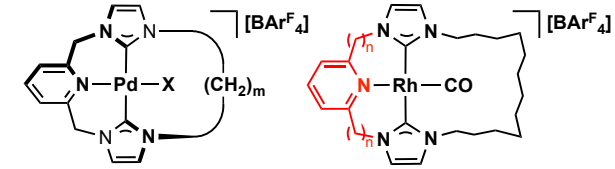


**D**; X = Cl, F; m = 8, 10, 12 **1a** (n = 1); **1b** (n = 0)

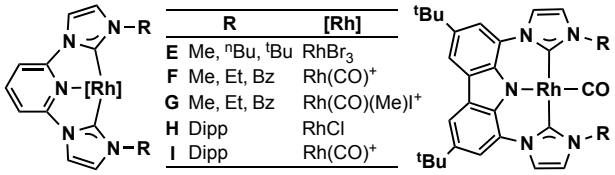


| | R | [Rh] |
|---|---|---|
| **E** | Me, $^n$Bu, $^t$Bu | $RhBr_3$ |
| **F** | Me, Et, Bz | $Rh(CO)^+$ |
| **G** | Me, Et, Bz | $Rh(CO)(Me)I^+$ |
| **H** | Dipp | RhCl |
| **I** | Dipp | $Rh(CO)^+$ |

**J** (R = Me, Et)

There are surprisingly few rhodium complexes containing neutral CNC pincer ligands as precedents for **1**. Indeed, those that have been reported are limited to a narrow range of pyridine-bridged systems (**E** – **I**, Chart 2).[12,13,14] Potentially tridentate bis(imidazolium)pyridine and bis(imidazolium)lutidine pro-ligands have also been observed to bridge two metal rhodium centres instead when using $[Rh(COD)Cl]_2$ (COD = cyclooctadiene) as the metal precursor.[12b,15] To avoid these bimetallic products, successful chelation procedures are characterised by relatively forcing reaction conditions (e.g. reflux in aerated acetonitrile, **E**)[12] or use of rhodium precursors with more readily displaced ligands; $[Rh(CO)_2(OAc)]_2$ (**F**)[13] and $[Rh(alkene)_2Cl]_2$ (alkene = cylcooctene, ethylene; **H**).[14] Closely related anionic carbazole-based rhodium CNC complexes (**J** in Chart 2) have been prepared by Kunz and co-workers and shown to undergo facile oxidative addition reactions with alkyl, allyl and benzyl halides.[16]

## Results and discussion

### Synthesis

Using our previously reported $Ag_2O$-based transmetallation strategy in combination with $[Rh(CO)_2Cl]_2$ and pre-formed macrocyclic pro-ligand **L1a**,[11] rhodium complex **1a** was obtained in a straightforward manner in good isolated yield (52%) following purification on silica and recrystallisation (Route 1, Scheme 1). This procedure results in the incorporation of the weakly coordinating $[BAr^F_4]^-$ counter anion ($Ar^F$ = 3,5-$C_6H_3(CF_3)_2$), which helps confer solubility in a range of organic solvents including diethyl ether, benzene and dichloromethane. Seeking to similarly prepare **1b**, we first attempted to prepare pyridine bridged **L1b**. Although we did not exhaustively investigate all potential macrocyclisation reactions, we found that direct adaption of routine literature protocols for non-cyclic CNC pro-ligands,[17] involving alkylation of 2,6-bis(imidazolyl)pyridine with 1,12-dibromododecane or alkylation of 1,12-bis(imidazolyl)dodecane with 2,6-dibromopyridine in refluxing dioxane, gave unsatisfactory results. Consequently to avoid the need for pre-formed macrocyclic pro-ligands **L1**, a metal-template based procedure employing more accessible terminal

alkene functionalised pro-ligands **L2** was developed (Route 2, Scheme 1). Macrocyclisation can be achieved using sequential olefin metathesis/hydrogenation steps following coordination of the pro-ligand. Methodology of this nature is well documented in the literature,[18] with work by Gladysz particularly noteworthy for its use of rhodium(I)-based templates.[19]

**Scheme 1**: Synthetic procedures for the preparation of **1** (a; n = 1; b, n = 0)[a]

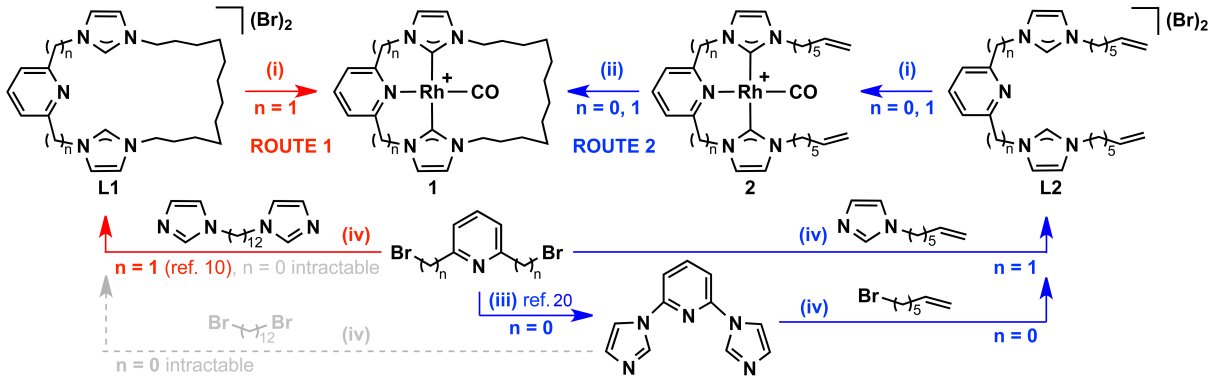


[a] $[BAr^F_4]^-$ anions omitted for clarity. Reagents and conditions: (i) $Ag_2O$ and $Na[BAr^F_4]$ then $[Rh(CO)_2Cl]_2$ ($CH_2Cl_2$, RT); (ii) [**2**] ~ 1 mmol $L^{-1}$; Grubbs I ($CH_2Cl_2$, RT), followed by hydrogenation using $[Ir(COD)(py)(PCy_3)][BAr^F_4]$ (10 mol%, 1 atm $H_2$, $CH_2Cl_2$, RT; n = 0) or Pd/C (20 mol%, 4 atm $H_2$, $CH_2Cl_2$, RT; n = 1); (iii) imidazole, $K_2CO_3$, DMF, 150°C [ref. 20]; (iv) 1,4-dioxane, reflux.

The terminal alkene functionalised pro-ligands (**L2**) were readily prepared and corresponding rhodium carbonyl adducts **2** generated using analogous reaction conditions to those used for **1a**. Purification on silica afforded **2a** (58%) and **2b** (83%) with good isolated yields. Macrocyclic derivatives **1** were then obtained from **2** by sequential olefin metathesis (Grubbs I) and hydrogenation. Under the same reaction conditions, analysis by ESI-MS revealed that the cyclisation of **2b** (100% conversion within 1 h) proceeded more rapidly than **2a** (ca. 69% conversion after 1 h). In both systems, complete and selective macrocyclisation is observed, however, the latter system required an additional portion of catalyst for full cyclisation. This difference in reactivity is entirely consistent with the more favourable ligand substituent geometry of the planar, pyridine-based **L2b** ligand. Hydrogenation of the resulting internal alkene groups using Pd/C (4 atm $H_2$) was effective for both systems, although under these conditions **1b** was found to be unstable.[21] Consequently, preparation of **1b** was instead carried out using $[Ir(COD)(py)(PCy_3)][BAr^F_4]$ as the catalyst,[22] enabling rapid and selective hydrogenation of the internal alkene group (10 mol% catalyst, 1 atm $H_2$). Ultimately despite these subtle differences in conditions, high purity samples of **1** were readily obtained from **2** in high isolated yields; 78% (**1a**) and 68% (**1b**) over two steps. With 2,6-bis(bromomethyl)pyridine as a common precursor, the effectiveness of each synthetic procedure can be evaluated for **1a**. Although the reactions were not fully optimised, route 2 noticeably gave a much greater overall yield (43% over four steps) in comparison to route 1 (20% over two steps); principally due to the low yielding preparation of **L1a** (39%) compared to **L2a** (94%).[11]

**Characterisation**

In $CD_2Cl_2$ solution **1a** is $C_2$ symmetric, with diagnostic diastereotopic resonances for the methylene bridge protons (py$C\underline{H}_2$) observed at δ 5.45 and 5.03 ($^2J_{HH}$ = 14.7 Hz) in the $^1$H NMR spectrum (298 K, 500 MHz); a geometry characteristic of lutidine-derived pincer ligands.[6,7,23] In line with preceding work using palladium,[11] this time averaged symmetry is fully retained on cooling to 185 K (see Figure S10). High symmetry is also adopted in a solid-state X-ray structure of **1a** obtained using single crystals grown from diethylether – hexane under an inert atmosphere (Figure 1, left). The ancillary carbonyl ligand notably binds with a Rh1-C2 bond distance of 1.804(3) Å and is well accommodated within the cavity of the macrocycle; the alkyl spacer only slightly askew. We have also obtained a much more asymmetric solid-state structure when crystallisation was carried out under non-routine conditions using a different solvent combination ($CH_2Cl_2$ – pentane, 1 atm CO). In this polymorph (**1a***), the alkyl spacer is instead completely twisted to one side of the molecule resulting in unmistakable $C_1$ symmetry (Figure 1, right). Despite the large difference in alkyl spacer conformation the structural metrics indicate the geometries about the rhodium centre are very similar; both show little distortion from square planar geometry with ideal sum of angles (360.1(5)º, **1a**; 360.2(12), **1a***) and essentially linear N10-Rh1-C2 bond angles (175.16(13)º, **1a**; 175.0(3)º, **1a***). Other key parameters are summarised in Table 1. We suggest the formation of the asymmetrical polymorph results from reversible carbon monoxide coordination during crystallisation, although we cannot rule out crystal packing effects.[24] Notwithstanding the origin of the polymorphism, the solid-state structures illustrate the full range of conformational flexibility accessible in the macrocyclic system. Ultimately in solution, the variable temperature NMR data clearly show that the carbonyl ligand does little to impede dynamic movement of the dodecamethylene spacer. A conclusion that is also supported by the similarity of spectroscopic data gathered for **1a** and non-cyclic **2a** (Table 1). Notably, no "macrocycle effect" is apparent on comparison of the carbenic and carbonyl $^{13}$C resonances (*ca* δ 182 ($^1J_{RhC}$ *ca* 40 Hz) and *ca* δ 194 ($^1J_{RhC}$ *ca* 80 Hz), respectively), and ν(CO) bands (**1a**, 1979 cm$^{-1}$; **2a** 1978 cm$^{-1}$ in $CH_2Cl_2$). Furthermore, despite different donor groups, data associated with the coordinated carbonyl ligand in **1a** is comparable with that found for phosphine pincer complex [Rh(PNP$^{tBu}$)(CO)]$^+$ (PNP$^{tBu}$ = 2,6-bis-(ditertbutylphosphinomethyl)pyridine); where the coordinated carbonyl ligand is characterised by $\delta_{13C}$ 196 ($^1J_{RhC}$ = 70 Hz) and ν(CO) 1982 cm$^{-1}$ in solution, and a Rh-C distance of 1.818(5) Å in the solid-state.[25]

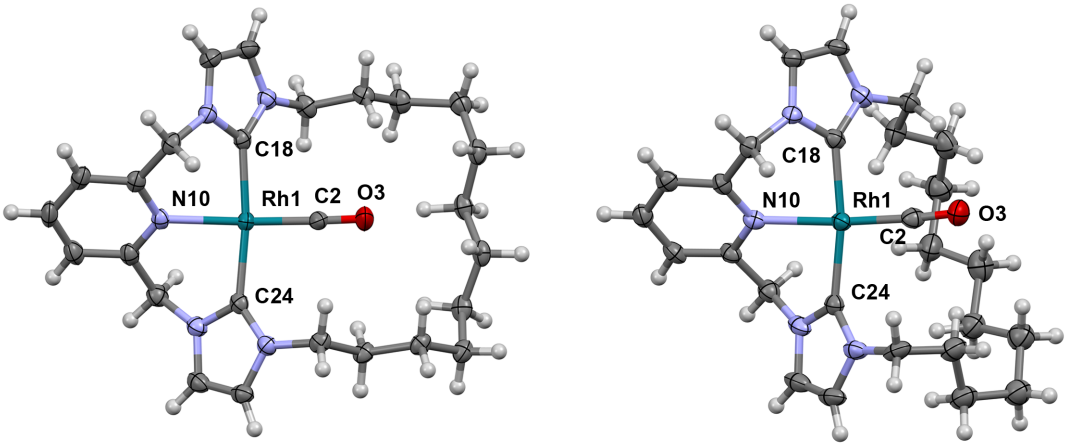


**Figure 1**: Solid-state structures of **1a/1a***. Thermal ellipsoids drawn at the 50% (left, symmetrical; **1a**) and 30% (right, asymmetrical; **1a***) probability levels; minor disordered components and anions are omitted for clarity. Selected bond lengths (Å) and angles(º): **1a** – Rh1-C2, 1.804(3); Rh1-N10, 2.134(2); Rh1-C18, 2.036(3); Rh1-C24, 2.042(3); C2-O3, 1.148(4); N10-Rh1-C2, 175.16(13); C18-Rh1-C24, 172.77(12); C11- C16-N17, 112.1(3). **1a*** – Rh1-C2, 1.796(9); Rh1-N10, 2.150(7); Rh1-C18, 2.020(7); Rh1-C24, 2.038(7); C2-O3, 1.153(11); N10-Rh1-C2, 175.0(3); C18-Rh1-C24, 169.9(3); C11-C16-N17, 110.8(6).

**Table 1**: Solution and solid-state characterisation metrics for **1** – **5**[a]

| | Ancillary ligands | ν(CO) /cm$^{-1}$ | $\delta_{\underline{C}O}$ ($J_{RhC}$ /Hz) | $\delta_{N\underline{C}N}$ ($J_{RhC}$ /Hz) | *r*(Rh**C**O) /Å | *r*(RhN) /Å | *r*(Rh**C**$_{CNC}$) /Å | ∠($C_{NCN}$Rh$C_{NCN}$) /º |
|---|---|---|---|---|---|---|---|---|
| **1a** | CO | 1979<br>1972[b] | 194.0 (80) | 181.8 (42) | 1.804(3);<br>1.796(9)[c] | 2.134(2);<br>2.150(7)[c] | 2.036(3), 2.042(3);<br>2.020(7), 2.038(7)[c] | 172.77(12);<br>169.9(3)[c] |
| **2a** | CO | 1978 | 193.9 (79) | 182.2 (41) | - | - | - | - |
| **3a** | (CO)(Me)I | 2067 | 189.4 (64) | 165.1 (34) | - | - | - | - |
| **4a** | $(CO)Cl_2$ | 2110 | 180.7 (57) | 160.1 (30) | - | - | - | - |
| **5**[b] | CO | 1929 | 197.4 (73) | 185.5 (43),<br>174.2 (44) | 1.799(3) | 2.113(2) | 2.048(3), 2.045(3) | 170.45(10) |
| **1b** | CO | 1986<br>1977[d] | 196.8 (78) | 186.5 (48) | 1.836(4) | 2.027(3) | 2.029(4), 2.028(4) | 155.18(15) |
| **2b** | CO | 1990<br>1980[d] | -[e] | 186.6 (48) | - | - | - | - |
| **3b** | (CO)(Me)I | 2070<br>2066[d] | 189.8 (61) | 180.2 (37) | 1.869(4) | 2.005(3) | 2.041(3), 2.028(3) | 156.47(15) |
| **4b** | $(CO)Cl_2$ | 2111 | 181.6 (57) | 173.9 (33) | 1.945(3) | 1.997(3) | 2.043(3), 2.049(3) | 156.47(12) |

[a] IR spectra recorded in $CH_2Cl_2$; NMR spectra recorded in $CD_2Cl_2$. [b] Measured in $C_6H_6$ (IR) or $C_6D_6$ (NMR). [c] Asymmetrical polymorph (**1a***). [d] Measured in MeCN. [e] Resonance not observed.

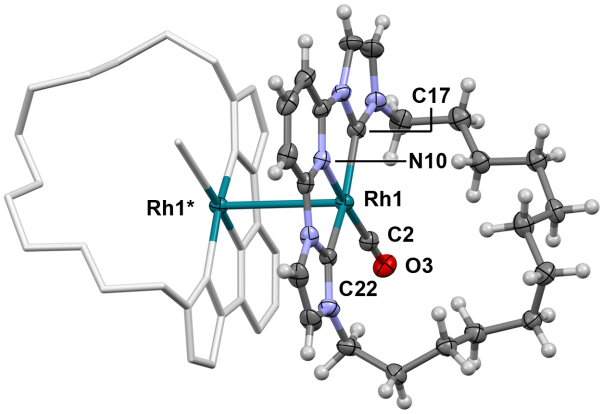


**Figure 2**: Solid-state structure of **1b**. Thermal ellipsoids drawn at 30% probability level; minor disordered components and anions are omitted for clarity; symmetry operation *-x*, *-y*+1, *-z*+1 was used to generate the stared atom. Selected bond lengths (Å) and angles(º): Rh1···Rh1*, 3.2758(6); Rh1-C2, 1.836(4); Rh1-N10, 2.027(3); Rh1-C17, 2.029(4); Rh1-C22, 2.028(4); C2-O3, 1.154(5); N10-Rh1-C2, 176.08(15); C17-Rh1-C22, 155.18(15).

Counteracting Coulombic repulsion, **1b** interestingly crystallises as a dimer with an unsupported Rh···Rh interaction (3.2758(6) Å) and the alkyl chain angled to one side (Figure 2). Metal-metal interactions of this nature have been documented for a variety of *planar* $d^8$ transition metal compounds and are attributed to overlap of $d_{z2}$ and $p_z$ orbitals on the adjacent metal centres.[26,27,28,29] For comparison, in both polymorphs of non-planar **1a**, the Rh···Rh distances are > 6.0 Å. The solid-state dimer of **1b** bears striking resemblance to that formed by macrocyclic $[Rh(SNS)(CO)]^+$ (SNS = 5,8,11-Trioxa-2,14-dithia[15]-(2,6)-pyridinophane), which is characterised by a Rh···Rh distance of 3.3320(6) Å and similar anti-orientation of the monomers about the metal-metal vector.[27] Similar metal-metal distances are also observed in related cationic rhodium(I) isocyanide dimers (3.19 – 3.29 Å)[29] which have been estimated to have a bond energy of up to 18 kcal·mol$^{-1}$.[30] In solution, the metal-metal interaction observed for **1b** in the solid-state is not retained, with concentration invariant UV-vis absorption spectra (deep violet in $CH_2Cl_2$ solution) and observation of $C_{2v}$ symmetry by NMR spectroscopy (298 K, 500 MHz). The high symmetry observed by NMR spectroscopy infers dynamic movement of the alkyl spacer across both sides of the molecule on the NMR time-scale and is only halted by cooling below 225 K, where decoalescence of the *N*-$CH_2C\underline{H_2}$ resonances can be noted (see Figure S13). The slow exchange limit cannot, however, be reached even on cooling to 185 K. ESI-MS revealed a parent ion signal at 508.1570 *m/z* (calc. 508.1578) with an integral-spaced isotope distribution, further supporting monomeric formulation of **1b** in solution. As seen with the lutidine-based ligands, spectroscopic data associated with the coordination of **L1b** and non-cyclic **L2b** are remarkably similar (Table 1). Likewise, reasonably good agreement is seen between **1b/2b** and **F**, based on the limited data available for the latter (ν(CO) 1977/1980 vs *ca* 1982 cm$^{-1}$ in MeCN).[13] In terms of the ability to form dimers in the solid-state, with no crystal structures at hand for **2b** and **F** (and to a lesser extent bulky **I**), it remains to be seen if this is a general feature of the chemistry of pyridine-based NHC pincers.

**Oxidative addition reactions**

As a means to assess differences in reactivity, we have studied oxidative addition reactions of **1** with MeI and $PhICl_2$ in $CD_2Cl_2$ solution by NMR spectroscopy (Scheme 2). Pyridine-based rhodium macrocyle **1b** reacted rapidly and quantitatively with MeI (3 eqv.) to afford yellow Rh(III) derivative **3b** within 3 h at 293 K. Under the same conditions, however, no significant reaction was apparent for **1a**, which instead required 50 eqv. MeI to promote oxidative addition (95% conversion to **3a** after 3 h). Scaling up the reaction, Rh(III) adduct **3b** was isolated in 75% yield. The structure of **3b** was firmly established by X-ray diffraction (Figure 3) and fully corroborated in solution by $^{1}H$, $^{13}C$ NMR and IR spectroscopy, in addition to ESI-MS and elemental analysis. An integral 3H doublet at δ 0.59 ($^{2}J_{RhH}$ = 2.1 Hz) in the $^{1}H$ NMR spectrum and low frequency $^{13}C$ doublet at δ -2.1 ($^{1}J_{RhC}$ = 18 Hz) are ascribed to the methyl ligand, which binds with a Rh1-C4 distance of 2.297(3) Å in the solid state. Moreover, the increase in formal oxidation state leads to reduced $^{1}J_{RhC}$ coupling constants for the NHC and carbonyl ligands (Table 1) and a significantly shifted ν(CO) band (2070 $cm^{-1}$ cf. 1986 $cm^{-1}$). Loss of symmetry as a consequence of MeI addition to **1b** is apparent both from the solid-state structure, the alkyl spacer of the macrocycle is notably skewed to one side of the complex, and NMR spectroscopy ($C_s$, 200 – 298 K, 500 MHz; Figure S18). In contrast to **3b**, our attempts to isolate pure **3a** were frustrated by the apparent instability of this species in the absence of excess MeI and samples of high purity could not be obtained: alongside reformation of **1a** by reductive elimination of MeI, a poorly characterised $C_1$ symmetric species was observed by $^{1}H$ NMR spectroscopy. Complex **3a** was therefore characterised *in situ*, in the presence of excess MeI. The formation of a single oxidative addition product is confirmed by a combination of $^{1}H$ ($\delta_{\underline{CH}3}$ 1.2, $^{2}J_{RhH}$ = 1.8 Hz) and $^{13}C$ ($\delta_{\underline{CH}3}$ -1.2, $^{2}J_{RhH}$ = 20 Hz) NMR spectroscopy, IR spectroscopy (ν(CO) = 2067 $cm^{-1}$) and ESI-MS ($[M]^{+}$ = 678.1169 (calc. 678.1171) *m/z*). We are unable to unambiguously assign the geometry of this product, but through comparison to the spectroscopic data of **3b**, the geometry of related literature precedents,[16] and noting the $C_2$ symmetry observed for **4a** (vide infra) we suggest the iodide and methyl ligands adopt a *trans* arrangement as is seen for **3b**. Significant dynamic behaviour of **3a** in solution is apparent by broad methylene resonances in the $^{1}H$ NMR spectrum at 298 K (500 MHz). Complete decoalescence is observed on cooling below 280 K and the exchange is frozen out at 250 K, revealing a $C_1$ geometry (see Figure S16). This dynamic behavior clearly indicates that, irrespective of the geometry of the ancillary ligands, the alkyl chain of the lutidine-based pincer ligand in **3b** is highly fluxional in solution.

**Scheme 2**: Reactions of **1** with MeI and $PhICl_2$.[a]

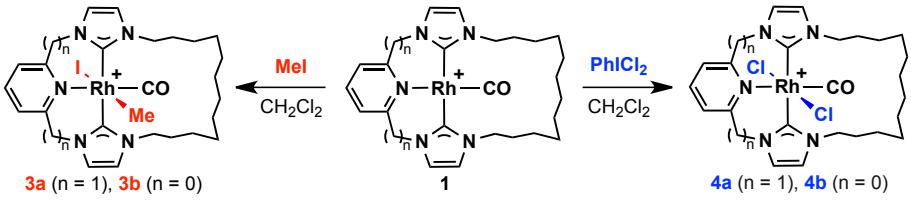


[a] $[BAr^{F}_4]^{-}$ anions omitted for clarity.

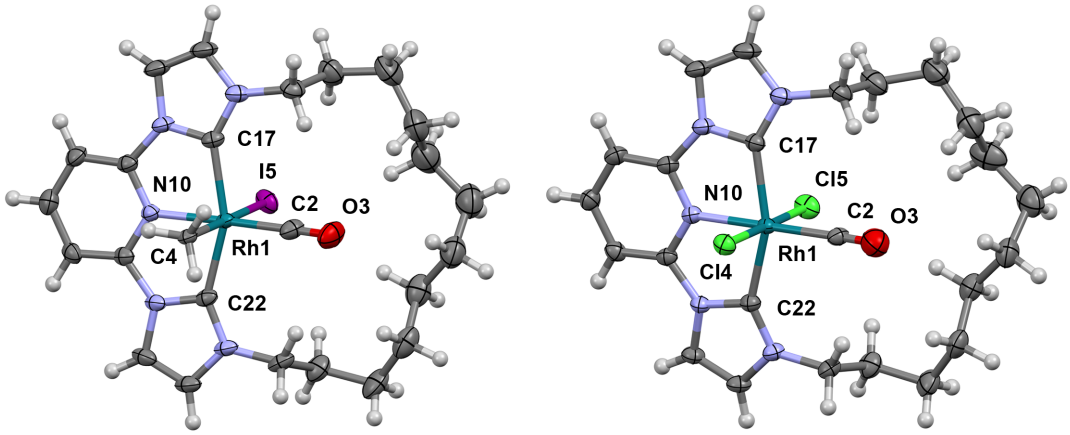


**Figure 3**: Solid-state structures of **3b** and **4b**. Thermal ellipsoids drawn at the 50% probability level; minor disordered components, solvent molecule and anions are omitted for clarity. Selected bond lengths (Å) and angles(º): **3b** – Rh1-C2, 1.869(4); Rh1-C4, 2.297(3); Rh1-I5, 2.7539(4); Rh1-N10, 2.005(3); Rh1-C17, 2.041(3); Rh1-C22, 2.028(3); C2-O3, 1.122(5); N10-Rh1-C2, 175.42(15); C4-Rh1-I5, 178.42(9); C17-Rh1-C22, 156.47(15); **4b** – Rh1-C2, 1.945(3); Rh1-Cl4, 2.3514(8); Rh1-Cl5, 2.3150(8); Rh1-N10, 1.997(3); Rh1-C17, 2.043(3); Rh1-C22, 2.049(3); C2-O3, 1.046(4); N10-Rh1-C2, 178.19(11); Cl4-Rh1-Cl5, 179.49(3); C17-Rh1-C22, 156.47(12).

Haynes and co-workers have previously studied the reaction kinetics of the closely related oxidative addition of MeI to **F** in acetonitrile; resulting in two isomeric Rh(III) species (**G**).[13] These reactions were shown to be second order and to proceed with large negative entropies of activation, consistent with a nucleophilic oxidative addition reaction mechanism. Given the structural similarity with **F** and extensive precedents in other $d^8$ systems, epitomised by Vaska's complex $[Ir(CO)Cl(PPh_3)_2]$,[31] this reaction mechanism also seems probable for the formation of **3** from **1**. In the absence of solid-state structures, Haynes and co-workers were unable to assign the geometry of the two isomers of **G**. By comparison of IR spectroscopic data for **3b** (ν(CO) = 2066 $cm^{-1}$ in MeCN), the major isomers of these products are readily assigned to species with the same stereoisomerism (ν(CO) *ca* 2072 $cm^{-1}$). The high selectively observed in the reaction of **1b** with MeI, in comparison to the non-macrocyclic systems **F**, is interesting and hints at a non-negligible steric role of the alkyl spacer during the reaction. Subtle electronic factors cannot be ignored, however, and notably selective *trans*-addition of alkyl halides is observed in the reaction of related, albeit neutral, **J**.[16]

Using the oxidant $PhICl_2$,[32] a trend begins to emerge in the reactivity characteristics of the two macrocyclic NHC systems. Although Rh(III) dichloride complexes **4** readily form on reaction of 1.1 equivalents of the oxidant with **1** (within 1 h), the lutidine-based derivative **4a** is unstable and appears to undergo a ligand redistribution reaction on attempted isolation, ultimately leading to intractable mixtures. Complex **4b** is in contrast stable and readily amenable to isolation (67% following crystallisation, Figure 3). In addition to the solid-state structure of **4b**, the structures of the Rh(III) dichlorides have been fully interrogated in solution by NMR and IR spectroscopy, in addition to ESI-MS – data for **4a** obtained *in situ*. Intact parent ion signals are observed in the ESI-MS spectra of both compounds: **4a**, 606.1271 (calc. 606.1268) *m*/*z*; **4b**, 578.0958

(calc. 578.0955) *m*/*z*. The adoption of a *trans*-configuration for the chloride ligands is apparent from high symmetry in the $^{1}$H NMR spectra of **4a** ($C_2$) and **4b** ($C_{2v}$) at 298 K (500 MHz). As for the parent compounds **1**, this high symmetry is only retained for the lutidine-based **4a** on cooling to 200 K (see Figures S21 and S23); the $^{1}$H NMR spectrum of **4b** at this temperature shows $C_s$ symmetry consistent with the skewing of the alkyl spacer to one side seen in the X-ray structure (Figure 3). As for the methyl iodide derivatives, the increase in formal state is accompanied by reduced $^{1}J_{RhC}$ coupling constants for the NHC and carbonyl ligands (Table 1) and a significantly shifted v(CO) band (**4a**, 2110 *cf.* 1979 cm$^{-1}$; **4b**, 2111 *cf.* 1986 cm$^{-1}$). The latter changes in the carbonyl stretching frequencies on oxidation are noticeably more pronounced in comparison to those seen during the formation of **3**.

The oxidative addition reactions clearly indicate an increase in reactivity (MeI) and product stability (MeI and $PhICl_2$) for the pyridine-based **1b** in comparison to the lutidine-based **1a**. Electronic differences between the two complexes are evident from the carbonyl stretching frequencies in $CH_2Cl_2$ (**1a**, 1979 cm$^{-1}$; **1b**, 1986 cm$^{-1}$), although the values do not tally with the observed trend in reactivity – the lower value observed for **1a** would conventionally suggest a more electron rich metal centre and a greater disposition towards oxidative addition.[31] Curiously, despite the differences between the two pincer architectures found for **1**, the carbonyl bands for the corresponding Rh(III) derivatives are, however, remarkably similar (**3a**, 2067 cm$^{-1}$; **3b**, 2070 cm$^{-1}$; **4a**, 2110 cm$^{-1}$; **4b**, 2111 cm$^{-1}$). Studying phosphine-based PNP rhodium systems, Milstein and co-workers have recently reported similar subtleties in the reactions of $[Rh(PNP^{R})(Me)I]^{+}$ (R = $^{t}$Bu, $^{i}$Pr) with carbon monoxide.[33] Rapid reductive elimination of MeI was observed in the PNP$^{t}$Bu-ligated system, whereas using the less bulky PNP$^{iPr}$ complex the Rh(III) adduct $[Rh(PNP^{iPr})(Me)I(CO)]^{+}$ could be isolated (although elimination of MeI occurs in the absence of a CO atmosphere). This reactivity strongly suggests that steric effects can play a key role in the relative stability of Rh(I) and Rh(III) fragments supported by tridentate ligands. Given the large changes in NHC-substituent geometry that result from the two central donor groups, evidenced by the highly dynamic movement of the alkyl spacer in the lutidine-based macrocyclic systems, the origin of the differences in reactivity observed between **1a** and **1b**, may be predominately steric in origin. In the absence of detailed calculations, however, the precise delineation of underlying steric or electronic effects remains to be determined.

**Dearomatisation of 1a**

In view of the low apparent stability of Rh(III) complexes of **L1a** and the increasing use of pincers as bifunctional ligands (*vide supra*), we sought to explore additional base-induced reactivity of **1a**. With rhodium PNP pincers **K** and ruthenium CNC pincers **L** as closely related precedents,[3,5b] the reaction of **1a** with $K[N(SiMe_3)_2]$ (1.1 eqv.) in $C_6D_6$ at 293 K was investigated (Scheme 3). A rapid reaction was evident by an immediate change in colour from yellow to deep red on mixing. Analysis by in-situ $^{1}$H NMR spectroscopy (298 K, 500 MHz) indicated the quantitative consumption of **1a** and formation of pyridine dearomatised **5**.

The formation of **5** is associated with very notable loss in symmetry ($C_1$) in comparison to **1a** ($C_2$) and the observation of $HN(SiMe_3)_2$ ($\delta_{CH3}$ = 0.10, $\delta_{NH}$ = -0.07) in the $^1H$ and $^{13}C$ NMR spectra. Broadened resonances are observed for the methylene protons at 298 K (500 MHz), which sharpen on cooling to 280 K (see Figure S26). At this temperature the vinylic proton is identified by a $^1H$ resonance at δ 5.81, alongside diastereotopic py$CH_2$ resonances (δ 3.72, 4.58; $^2J_{HH}$ = 13 Hz) and two sets of similarly diastereotopic *N*-$CH_2$ resonances. Heating the sample to 350 K results in coalescence of the methylene signals and time-averaged $C_s$ symmetry, resulting from atropisomerisation of the pincer backbone *and* coupled dynamics of the dodecamethylene spacer. The imidazolylidene (4×1H) and pyridine (3×1H) resonances remain sharp across the full temperature range measured (280 – 350 K). Complex **5** is highly reactive and best prepared and characterised *in situ*. Small quantities of **5** can be isolated from benzene by decantation (to remove precipitated $K[BAr^F_4]$) and layering with rigorously dried pentane (52% yield). Using this method we have obtained single crystalline samples suitable for X-ray diffraction analysis; the resulting solid-state structure is depicted in Figure 4. Crystallographically characterised examples of group 9 dearomatised pincer complexes are scarce.[34,35] In comparison to the precursor **1a**, the presence of an $sp^2$ carbon in the pincer backbone of **5** is readily apparent by a marked increase in the C11-C16-N17 angle (from 112.1(3)/110.8(6)º to 126.7(3)) and contraction of the C11-C16 bond (from 1.506(5)/1.502(10) Å to 1.356(4) Å; *ca* 0.15 Å). A similar but less pronounced bond length change was also observed on dearomatisation of $[Rh(SNN)(CO)]^+$ (**M**; SNN = 2-(diethylaminomethyl)-6-(*tert*-butylsulfinylmethyl)pyridine); from 1.502(4) to 1.391(5) Å; ca. 0.11 Å).[34] Dearomatisation of the CNC pincer backbone is readily apparent by bond length alternation in the pyridine ring, which is illustrated in the insert of Figure 4. The resulting amido group is associated with a slightly shortened Rh1-N10 bond (2.113(2) Å, cf. 2.134(2)/2.150(7) Å for **1a**), but more noticeably, a low frequency carbonyl band in the IR spectrum measured in $C_6H_6$ (1929 $cm^{-1}$ cf. 1972 $cm^{-1}$ for **1a**).

**Scheme 3**: Formation of **5** and closely related literature precedents.[a]

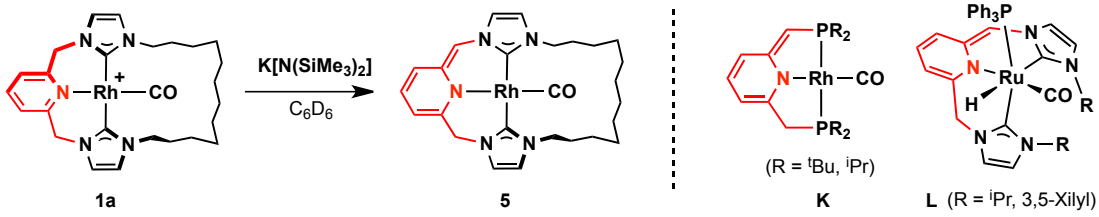


**1a** **5** **K** **L** (R = $^i$Pr, 3,5-Xilyl)

[a] $[BAr^F_4]^-$ anion omitted for clarity.

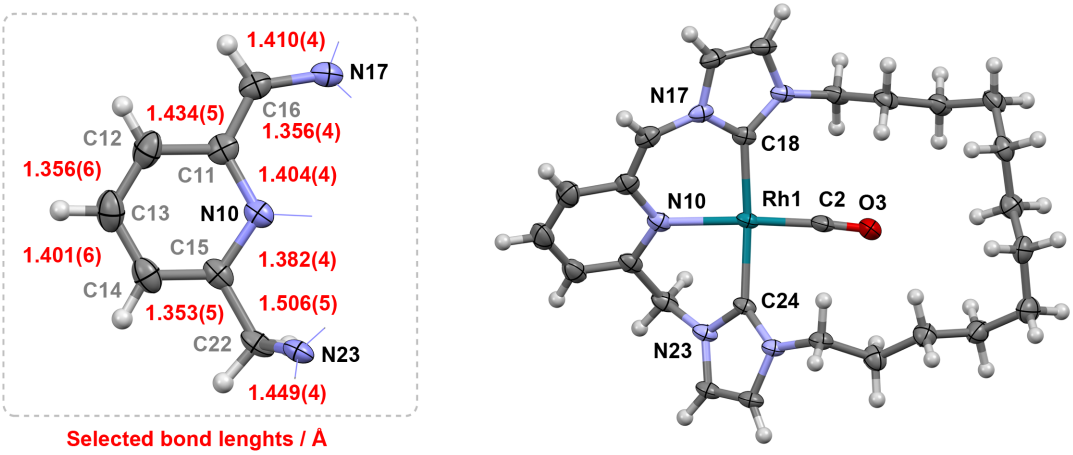


**Figure 4**: Solid-state structure of **5**. Thermal ellipsoids drawn at the 30% probability level; minor disordered components and solvent omitted for clarity. Additional bond lengths (Å) and angles(º): Rh1-C2, 1.799(3); Rh1-N10, 2.113(2); Rh1-C18, 2.048(3); Rh1-C24, 2.045(3); C2-O3, 1.149(4); N10-Rh1-C2, 172.88(11); C18-Rh1-C24, 170.45(10); C11-C16-N17, 126.7(3); C15-C22-N23, 111.3(2).

**Summary**

Building upon our previous work with palladium,[11] in this report we have described the preparation and reactivity of rhodium complexes containing macrocyclic CNC pincer ligands. In particular, we have developed a general synthetic procedure employing readily accessed terminal alkene functionalised pro-ligands that entails sequential $Ag_2O$-based transmetallation, ring-closing olefin metathesis and hydrogenation. This general procedure overcomes difficulties relating to the preparation of pre-formed macrocyclic pro-ligands and enabled access to both lutidine- ($[Rh(C^N^C\text{-}(CH_2)_{12})(CO)]^+$, **1a**) and pyridine-($[Rh(CNC\text{-}(CH_2)_{12})(CO)]^+$, **1b**) based rhodium macrocycles in high purity and with good isolated yields. Indeed, in the case of the lutidine-based system, where a pre-formed macrocyclic pro-ligand can be prepared, the macrocyclisation procedure is twice as high yielding overall despite double the number of steps. Altering the geometry of the pincer backbone results in marked differences in spectroscopic characteristics, overall structural dynamics and chemical reactivity. The lutidine-based CNC systems are characterised by increased fluxional motion of the macrocycles' dodecamethylene spacer in comparison to the pyridine-based analogues. In solution **1a** shows temperature invariant time averaged $C_2$ symmetry by $^1$H NMR spectroscopy ($CD_2Cl_2$, 500 MHz), while in the solid-state two polymorphs can be obtained showing different conformations of the alkyl spacer about the metal-carbonyl bond (asymmetric and symmetric). In contrast, time-averaged motion of alkyl spacer in **1b** can be halted by cooling below 225 K ($CD_2Cl_2$, 500 MHz) and the complex crystallises as a dimer with an interesting unsupported Rh···Rh bonding interaction (3.2758(6) Å). These structural variations also appear to be manifested in the reactivity of the complexes, with reaction of MeI and $PhICl_2$ leading to stable isolable Rh(III) products for **1b** only. Although the corresponding Rh(III) adducts resulting from **1a** are ultimately unstable, the backbone of the pincer can be dearomatised by addition of $K[N(SiMe_3)_2]$ accessing potential bifunctional reactivity not possible with **1b**. The resulting neutral dearomatised complex ($[Rh(C^N^C^*\text{-}(CH_2)_{12})(CO)]$, **5**) has been fully characterised in

solution, by variable temperature $^{1}$H NMR spectroscopy, and in the solid-state, by X-ray diffraction. Further investigation of the coordination and organometallic chemistry of macrocyclic CNC and CCC pincer ligands, including **1**, is on-going in our laboratory.

## Experimental

### General experimental methods

Manipulations were performed under an inert atmosphere using Schlenk (dinitrogen unless otherwise stated) and glove box (argon) techniques unless otherwise stated. Glassware was oven dried at 130ºC overnight and flamed under vacuum prior to use. Anhydrous solvents (<0.005% $H_2O$) were purchased from Acros Organics or Sigma-Aldrich and used as supplied: DMF, MeCN, $CH_2Cl_2$, THF, 1,4-dioxane, hexane, pentane and $Et_2O$. $CD_2Cl_2$ was dried over $CaH_2$, vacuum distilled and stored under argon. $C_6D_6$ was dried over sodium, vacuum distilled and stored under argon. $Na[BAr^F{}_4]$[36], $[Rh(CO)_2Cl]_2$,[37] **L1a**[11], 2,6-bis(imidazolyl)pyridine[20] and $[Ir(COD)(py)(PCy_3)][BAr^F{}_4]$[22] were synthesised using literature procedures. All other solvents and reagents are commercial products and were used as received. NMR spectra were recorded on Bruker DPX-400, AV-400, DRX-500 and AV-600 spectrometers at 298 K unless otherwise stated. Chemical shifts are quoted in ppm and coupling constants in Hz. IR spectra were recorded on a Perkin-Elmer Spectrum One FT-IR spectrometer. UV-vis absorption spectra were recorded on Agilent Cary 60 spectrometer. High resolution ESI-MS were recorded on a Bruker MaXis spectrometer. Microanalyses were performed at the London Metropolitan University by Stephen Boyer.

### Synthesis of new compounds

#### *7-imidazole-1-heptene*

NaH (60% wt suspension in mineral oil, 0.32 g, 8.03 mmol) was added portion-wise to a stirred solution of imidazole (0.50 g, 7.34 mmol) in 50 mL THF at 0°C, over 5 minutes. 7-bromo-1-heptene (1.18 mL, 7.73 mmol) was then added via syringe. The mixture was heated at reflux for 16 hours and then quenched by addition of $H_2O$, after cooling to room temperature. The product was extracted with $CH_2Cl_2$ (3 x 50 mL) and the combined organic extracts were washed with $H_2O$ and then dried over $Na_2SO_4$. The crude product (yellow oil) was then purified by silica column chromatography (10% MeOH in $CH_2Cl_2$) to yield the pure product as a colourless oil. Yield: 0.880 g (46%). **$^{1}$H NMR** (300 MHz, $CDCl_3$): δ 7.45 (s, 1H, imid), 7.05 (s, 1H, imid), 6.90 (s, 1H, imid), 5.77 (ddt, $^{3}J_{HH}$ = 16.9, 9.9, 6.6, 1H, C<u>H</u>=$CH_2$), 4.90 – 5.07 (m, 2H, CH=C<u>H</u>$_2$), 3.92 (t, $^{3}J_{HH}$ = 7.1, 2H, *N*-$CH_2$), 1.98 – 2.09 (m, 2H, $CH_2$), 1.78 (app. pent, *J* = 7, 2H, $CH_2$), 1.22 – 1.49 (m, 4H, $CH_2$). **$^{13}$C{$^{1}$H} NMR** (75 MHz, $CDCl_3$): δ 138.5, 137.2, 129.5, 118.9, 114.9, 47.1, 33.6, 31.1, 28.4, 26.1. **ESI-MS** ($CH_3CN$, 180 °C, 3 kV): positive ion: 165.1391 *m/z*, $[M]H^+$ (calc. 165.1386). **Anal**. Calcd for $C_{10}H_{16}N_2$ (164.25 g $mol^{-1}$): C, 73.13; H, 9.82; N, 17.06. Found: C, 72.97; H, 9.68; N, 16.96.

***C^N^C-((CH$_2$)$_5$CH=CH$_2$)$_2$ (L2a)***

A mixture of 2,6-bis(bromomethyl)pyridine (1.30 g, 4.90 mmol) and 7-imidazole-1-heptene (2.41 g, 14.7 mmol) in 1,4-dioxane (50 mL) was heated at reflux for 5 hours. The solvent was removed *in vacuo* to give an orange oil, which was then extracted with MeCN (50 mL). The filtrate was reduced in volume and excess $Et_2O$ added to separate the product as an oil, which was separated by decantation. The remaining oil was washed with $Et_2O$ (3 x 50 mL) before drying in vacuo to a yield a yellow foam. Yield: 2.737 g (94%). **$^1$H NMR** (400 MHz, $CDCl_3$): δ 10.51 (b, 2H, imid), 8.17 (app. t, *J* = 2, 2H, imid), 7.73 (d, $^3J_{HH}$ = 7.6, 2H, py), 7.62 (dd, $^3J_{HH}$ = 8.3, 7.1, 1H, py), 7.37 (app. t, *J* = 2, 2H, imid), 5.73 (s, 4H, pyC$\underline{H}_2$), 5.65 (ddt, $^3J_{HH}$ = 16.9, 10.1, 6.7, 2H, C$\underline{H}$=CH$_2$), 4.88 (d app. q, $^3J_{HH}$ = 16.9, *J* = 2, 2H, CH=C$\underline{H}_2$), 4.83 (br d, $^3J_{HH}$ = 10.1, 2H, CH=C$\underline{H}_2$), 4.34 (t, $^3J_{HH}$ = 7.5, 4H, *N*-C$\underline{H}_2$CH$_2$), 1.94 (app. q, *J* = 7, 4H, CH$_2$), 1.86 (app. pent, *J* = 8, 4H, CH$_2$), 1.20 – 1.40 (m, 8H, CH$_2$). **$^{13}$C{$^1$H} NMR** (101 MHz, $CDCl_3$): δ 153.3, 139.1, 138.2, 137.2, 137.1, 124.0, 123.9, 121.5, 115.0, 53.4, 50.1, 33.4, 30.3, 28.2, 25.6. **ESI-MS** ($CH_3CN$, 180 °C, 3 kV): positive ion: 216.6598 *m/z*, $[M]^{2+}$ (calc. 216.6597). **Anal**. Calcd for $C_{27}H_{39}Br_2N_5$ (593.44 g mol$^{-1}$): C, 54.65; H, 6.62; N, 11.80. Found: C, 54.49; H, 6.57; N, 11.74.

***[Rh(C^N^C-((CH$_2$)$_5$CH=CH$_2$)$_2$)(CO)][BAr$^F_4$] (2a)***

A mixture of **L2a** (0.050 g, 0.084 mmol), $Ag_2O$ (0.020 g, 0.084 mmol) and Na[BAr$^F_4$] (0.075 g, 0.084 mmol) in $CH_2Cl_2$ (3 mL) was stirred in the absence of light for 16 hours. A solution of $[Rh(CO)_2Cl]_2$ (0.016 g, 0.042 mmol) in $CH_2Cl_2$ (3 mL) was added and the resulting suspension stirred for a further 20 hours. The suspension was filtered through a pad of silica, eluting with $CH_2Cl_2$, to yield the crude product upon removal of solvent. The crude material was then purified by precipitation from $Et_2O$ – pentane, to yield the pure product as a yellow powder. Yield: 0.070 g (58%). **$^1$H NMR** (400 MHz, $CD_2Cl_2$): δ 7.86 (t, $^3J_{HH}$ = 7.7, 1H, py), 7.70 – 7.75 (m, 8H, Ar$^F$), 7.55 (br, 4H, Ar$^F$), 7.49 (d, $^3J_{HH}$ = 7.7, 2H, py), 7.14 (d, $^3J_{HH}$ = 1.9, 2H, imid), 6.99 (d, $^3J_{HH}$ = 2.0, 2H, imid), 5.75 (ddt, $^3J_{HH}$ = 16.9, 10.2, 6.7, 2H, C$\underline{H}$=CH$_2$), 5.46 (d, $^2J_{HH}$ = 14.7, 2H, pyC$\underline{H}_2$), 5.02 (d, $^2J_{HH}$ = 14.7, 2H, pyC$\underline{H}_2$), 4.94 (d app. q, $^3J_{HH}$ = 16.9, *J* = 2, 2H, CH=C$\underline{H}_2$), 4.89 (br d, $^3J_{HH}$ = 10.2, 2H, CH=C$\underline{H}_2$), 4.13 (t, $^3J_{HH}$ = 7.6, 4H, *N*-C$\underline{H}_2$CH$_2$), 2.02 (app. q, *J* = 7, 4H, CH$_2$), 1.82 – 1.95 (m, 4H, CH$_2$), 1.30 – 1.48 (m, 8H, CH$_2$). **$^{13}$C{$^1$H} NMR** (101 MHz, $CD_2Cl_2$): δ 193.9 (d, $^1J_{RhC}$ = 79, carbonyl), 182.2 (d, $^1J_{RhC}$ = 41, carbene), 162.2 (q, $^1J_{CB}$ = 49, Ar$^F$), 156.0 (s, py), 141.4 (s, py), 139.1 (s, $\underline{C}$H=CH$_2$), 135.3 (s, Ar$^F$), 129.3 (q, $^2J_{CF}$ = 32, Ar$^F$), 125.1 (q, $^1J_{CF}$ = 272, Ar$^F$), 124.8 (s, py), 121.8 (s, imid), 121.3 (s, imid), 118.0 (sept, $^3J_{FC}$ = 4, Ar$^F$), 114.8 (s, CH=$\underline{C}$H$_2$), 55.8 (s, py$\underline{C}$H$_2$), 51.4 (s, *N*-$\underline{C}$H$_2$CH$_2$), 34.0 (s, CH$_2$), 31.7 (s, CH$_2$), 28.8 (s, CH$_2$), 26.5 (s, CH$_2$). **ESI-MS** ($CH_3CN$, 180 °C, 3 kV): positive ion: 562.2067 *m/z*, $[M]^+$ (calc. 562.2048). **Anal**. Calcd for $C_{60}H_{49}BF_{24}N_5ORh$ (1425.74 g mol$^{-1}$): C, 50.55; H, 3.46; N, 4.91. Found: C, 50.43; H, 3.36; N, 4.90. **IR** ($CH_2Cl_2$): *ν*(CO) 1978 cm$^{-1}$.

***[Rh(C^N^C-(CH$_2$)$_{12}$)(CO)][BAr$^F_4$] (1a)***

*Route 1*: A mixture of **L1a** (0.100 g, 0.176 mmol), $Ag_2O$ (0.041 g, 0.176 mmol) and Na[BAr$^F_4$] (0.170 g, 0.192 mmol) in $CH_2Cl_2$ (3 mL) was stirred in the absence of light for 16 hours. A solution of $[Rh(CO)_2Cl]_2$ (0.034 g, 0.088 mmol) in $CH_2Cl_2$ (3 mL) was added and the suspension stirred for a further 5 hours. The solution was

filtered and the filtrate reduced to dryness to afford the crude product, which was then passed through a silica pad using $CH_2Cl_2$ as the eluent to give a vibrant yellow oil. The oil was then dissolved in $Et_2O$ and excess hexane added to precipitate the product, which was isolated by filtration and washed with hexane to give **1a** as a yellow powder. Yield: 0.129 g (52%).

*Route 2:* $N_2$ was bubbled through a solution of **2a** (0.100 g, 0.070 mmol) and Grubbs I (0.003 g, 0.004 mmol) in $CH_2Cl_2$ (70 mL) for 1 h. After this time, ESI-MS indicated 69% reaction conversion. A further portion of Grubbs I (0.003 g, 0.004 mmol) was added and $N_2$ bubbled through for an additional hour, at which time ESI-MS indicated the reaction had gone to completion. The resulting solution was concentrated and passed through a silica pad using $CH_2Cl_2$ as the eluent to afford [Rh(C^N^C-$C_{12}H_{22}$)(CO)][$BAr^F_4$] as a yellow glass (cis:trans ~ 1:3). Yield: 0.096 g (95%). A solution of [Rh(C^N^C-$C_{12}H_{22}$)(CO)][$BAr^F_4$] (0.096 g, 0.065 mmol) in $CH_2Cl_2$ (5 mL) was added to a J. Young's flask charged with palladium on carbon (10 wt% Pd, 0.014 g, 0.013 mmol, ca. 20 mol% Pd) and the solution placed under $H_2$ (4 bar). After stirring for 72 h, the reaction mixture was degassed, concentrated and filtered through a celite pad. The filtrate was concentrated in vacuo to give **1a** as a yellow-orange foam. Yield: 0.075 g (82%).

Data for [Rh(C^N^C-$C_{12}H_{22}$)(CO)][$BAr^F_4$]: **$^1$H NMR** (400 MHz, $CD_2Cl_2$, trans isomer only): δ 7.88 (t, $^3J_{HH}$ = 7.7, 1H, py), 7.70 – 7.75 (m, 8H, $Ar^F$), 7.55 (br, 4H, $Ar^F$), 7.50 (d, $^3J_{HH}$ = 7.7, 2H, py), 7.15 (d, $^3J_{HH}$ = 1.9, 2H, imid), 7.01 (d, $^3J_{HH}$ = 1.9, 2H, imid), 5.40 (br, 2H, py$C\underline{H}_2$), 5.35 – 5.39 (m, 2H,CH=CH), 5.03 (br, 2H, py$C\underline{H}_2$), 3.90 – 4.36 (m, 4H, *N*-$C\underline{H}_2CH_2$), 1.14 – 2.24 (m, 16H, $CH_2$). **ESI-MS** ($CH_3CN$, 180 °C, 3 kV): positive ion: 534.1762 m/z, $[M]^+$ (calc. 534.1735). Data for **1a**: **$^1$H NMR** (500 MHz, $CD_2Cl_2$): δ 7.88 (t, $^3J_{HH}$ = 7.7, 1H, py), 7.70 – 7.75 (m, 8H, $Ar^F$), 7.56 (br, 4H, $Ar^F$), 7.51 (d, $^3J_{HH}$ = 7.7, 2H, py), 7.14 (d, $^3J_{HH}$ = 1.9, 2H, imid), 7.00 (d, $^3J_{HH}$ = 1.9, 2H, imid), 5.45 (d, $^2J_{HH}$ = 14.7, 2H, py$C\underline{H}_2$), 5.03 (d, $^2J_{HH}$ = 14.7, 2H, py$C\underline{H}_2$), 4.25 – 4.36 (m, 2H, *N*-$C\underline{H}_2$CH2), 3.93 – 4.04 (m, 2H, *N*-$CH_2$), 1.77 – 2.01 (m, 4H, $CH_2$), 1.10 – 1.53 (m, 16H, $CH_2$). **$^{13}$C{$^1$H} NMR** (101 MHz, $CD_2Cl_2$): δ 194.0 (d, $^1J_{RhC}$ = 80, carbonyl), 181.8 (d, $^1J_{RhC}$ = 42, carbene), 162.3 (q, $^1J_{BC}$ = 50, $Ar^F$), 156.0 (s, py), 141.5 (s, py), 135.4 (s, $Ar^F$), 129.4 (q, $^2J_{CF}$ = 32, $Ar^F$), 125.2 (q, $^1J_{CF}$ = 273, $Ar^F$), 124.9 (s, py), 121.9 (s, imid), 121.5 (s, imid), 118.0 (sept, $^3J_{FC}$ = 4, $Ar^F$), 55.9 (s, py$\underline{C}H_2$), 51.5 (s, *N*-$\underline{C}H_2CH_2$), 31.6 (s, $CH_2$), 28.0 (s, $CH_2$), 27.9 (s, $CH_2$), 27.9 (s, $CH_2$), 24.6 (s, $CH_2$). **ESI-MS** ($CH_3CN$, 180 °C, 3 kV): positive ion: 536.1903 *m/z*, $[M]^+$ (*calc.* 536.1891). **Elemental** Anal. Calcd for $C_{58}H_{47}BF_{24}N_5ORh$ (1399.70 g $mol^{-1}$): C, 49.77; H, 3.38; N, 5.00. Found: C, 49.92; H, 3.40; N, 5.21. **IR** ($CH_2Cl_2$): ν(CO) 1979 $cm^{-1}$. **IR** ($C_6H_6$): ν(CO) 1972 $cm^{-1}$.

***CNC-((CH$_2$)$_5$CH=CH$_2$)$_2$ (L2b)***

A mixture of 2,6-bis(imidazolyl)pyridine (0.634 g, 2.77 mmol) and 7-bromo-1-heptene (1.05 mL, 6.91 mmol) in 1,4-dioxane (2 mL) was stirred at 100°C in a sealed Young's flask for 16 hours. After cooling, the reaction mixture was extracted with MeCN (3 x 10 mL). To the filtrate was added $Et_2O$ (20 mL) to form a white suspension, which was left to stand for 4 hours before filtration. The remaining white solid was washed

with $Et_2O$ and dried in vacuo to give the product. Yield: 1.067 g (68%). **$^1$H NMR** (300 MHz, $CDCl_3$): δ 11.92 (bs, 2H, imid), 9.27 (app. t, *J* = 2, 2H, imid), 8.78 (d, $^3J_{HH}$ = 8.2, 2H, py), 8.31 (t, $^3J_{HH}$ = 8.1, 1H, py), 7.52 (app. t, *J* = 2, 2H, imid), 5.75 (ddt, $^3J_{HH}$ = 16.9, 10.1, 6.7, 2H, C<u>H</u>=$CH_2$), 4.98 (d app. q, $^3J_{HH}$ = 16.9, *J* = 2, 2H, CH=C<u>H</u>$_2$), 4.93 (br d, $^3J_{HH}$ = 10.1, 2H, CH=C<u>H</u>$_2$), 4.59 (t, $^3J_{HH}$ = 7.3, 4H, *N*-$CH_2$), 1.95 – 2.12 (m, 8H, $CH_2$), 1.34 – 1.54 (m, 8H, $CH_2$). **$^{13}$C{$^1$H} NMR** (75 MHz, $CDCl_3$): δ 145.4, 145.3, 138.3, 136.7, 123.3, 120.9, 115.6, 115.1, 50.9, 33.4, 30.3, 28.2, 25.7. **ESI-MS** ($CH_3CN$, 180 °C, 3 kV): positive ion: 202.6458 *m/z*, $[M]^{2+}$/2 (calc. 202.6441). **Anal.** Calcd for $C_{25}H_{35}Br_2N_5$ (565.39 g $mol^{-1}$): C, 53.11; H, 6.24; N, 12.39. Found: C, 52.92; H, 6.11; N, 12.28.

***[Rh(CNC-((CH$_2$)$_5$CH=CH$_2$)$_2$)(CO)][BAr$^F_4$] (2b)***

A mixture of **L2b** (0.100 g, 0.177 mmol), $Ag_2O$ (0.041 g, 0.176 mmol) and Na[$BAr^F_4$] (0.173 g, 0.195 mmol) in $CH_2Cl_2$ (2 mL) was stirred in the absence of light for 16 hours. The reaction mixture was filtered onto $[Rh(CO)_2Cl]_2$ (0.035 g, 0.088 mmol) and the resulting suspension stirred for a further 5 minutes before further filtration. The filtrate was reduced to dryness and purified on silica ($CH_2Cl_2$) to afford the product as a purple foam on removal of the solvent. Yield: 0.218 g (83%). **$^1$H NMR** (400 MHz, $CD_2Cl_2$): δ 8.01 (t, $^3J_{HH}$ = 8.2, 1H, py), 7.72 – 7.80 (m, 8H, $Ar^F$), 7.58 (br, 4H, $Ar^F$), 7.43 (d, $^3J_{HH}$ = 2.2, 2H, imid), 7.15 (d, $^3J_{HH}$ = 8.2, 2H, py), 7.10 (d, $^3J_{HH}$ = 2.2 Hz, 2H, imid), 5.81 (ddt, $^3J_{HH}$ = 16.9, 10.2, 6.7 Hz, 2H, C<u>H</u>=$CH_2$), 5.00 (d app. q, $^3J_{HH}$ = 16.9, *J* = 2, 2H, CH=C<u>H</u>$_2$), 4.95 (br d, $^3J_{HH}$ = 10.2, 2H, CH=C<u>H</u>$_2$), 4.14 (t, $^3J_{HH}$ = 7.5, 4H, *N*-$CH_2$), 2.08 (app. q, *J* = 7, 4H, $CH_2$), 1.93 (app. pent, *J* = 7, 4H, $CH_2$), 1.38 – 1.54 (m, 8H, $CH_2$). **$^{13}$C{$^1$H} NMR** (101 MHz, $CD_2Cl_2$): δ 186.6 (d, $^1J_{RhC}$ = 48, carbene), 162.4 (q, $^1J_{CB}$ = 50, $Ar^F$), 152.7 (s, py), 146.3 (s, py), 139.0 (s, <u>C</u>H=$CH_2$), 135.4 (s, $Ar^F$), 129.5 (q, $^2J_{FC}$ = 32, $Ar^F$), 125.2 (q, $^1J_{FC}$ = 272, $Ar^F$), 123.8 (s, imid), 118.1 (sept, $^3J_{FC}$ = 4, $Ar^F$), 117.0 (s, imid), 115.0 (s, CH=<u>C</u>H$_2$), 106.7 (s, py), 53.0 (s, *N*-$CH_2$), 34.0 (s, $CH_2$), 31.6 (s, $CH_2$), 28.8 (s, $CH_2$), 26.4 (s, $CH_2$); carbonyl resonance not observed. **ESI-MS** ($CH_3CN$, 180 °C, 3 kV): positive ion: 534.1726 *m/z*, $[M]^+$ (calc. 534.1735). **Anal.** Calcd for $C_{58}H_{45}BF_{24}N_5ORh$ (1397.69 g $mol^{-1}$): C, 49.84; H, 3.25; N, 5.01. Found: C, 49.72; H, 3.25; N, 5.12. **IR** ($CH_2Cl_2$): ν(CO) 1990 $cm^{-1}$. **IR** ($CH_3CN$): ν(CO) 1980 $cm^{-1}$.

***[Rh(CNC-(CH$_2$)$_{12}$)(CO)][BAr$^F_4$] (1b)***

$N_2$ was bubbled through a solution of **2b** (0.100 g, 0.074 mmol) and Grubbs I (0.003 g, 0.004 mmol) in $CH_2Cl_2$ (70 mL) for 30 minutes (reaction completion observed by ESI-MS). The resulting solution was concentrated to dryness and purified on silica ($CH_2Cl_2$). [Rh(CNC-$C_{12}H_{22}$)(CO)][$BAr^F_4$] (cis:trans ~ 1:1) was obtained as a purple powder by precipitation from $CH_2Cl_2$ with excess pentane and subsequent filtration. Yield: 0.083 g (82%). A solution of [Rh(CNC-$C_{12}H_{22}$)(CO)][$BAr^F_4$] (0.050 g, 0.037 mol) and [Ir(COD)(py)($PCy_3$)][$BAr^F_4$] (0.003 g, 0.004 mol) in $CH_2Cl_2$ (2 mL) was placed under hydrogen (1 bar). After stirring for 2 hours the reaction mixture was concentrated in vacuo. The residue was then purified on silica ($CH_2Cl_2$). The eluted solvent was concentrated to 2 mL before precipitation of the product with excess pentane. Complex **2b** as a dark green powder was obtained by filtration and washed with pentane (3 x 5 mL). Yield: 0.042 g (83%).

Data for [Rh(CNC-$C_{12}H_{22}$)(CO)][$BAr^F_4$]: **$^1$H NMR** (400 MHz, $CD_2Cl_2$): δ 8.04 (t, $^3J_{HH}$ = 8.2, 1H, py), 7.70 – 7.75 (m, 8H, $Ar^F$), 7.56 (s, 4H, $Ar^F$), 7.48/7.49 (d, $^3J_{HH}$ = 2.3, 2H, imid), 7.17 (d, $^3J_{HH}$ = 8.1, 2H, py), 7.09/7.10 (d, $^3J_{HH}$ = 2.3, 2H, imid), 5.27 – 5.37 (m, 2H, CH=CH), 4.13 – 4.21 (m, 4H, *N*-$CH_2$), 1.97 – 2.09 (m, 4H, $CH_2$), 1.80 – 1.91 (m, 4H, $CH_2$), 1.24 – 1.50 (m, 8H, $CH_2$). **ESI-MS** ($CH_3CN$, 180°C, 3 kV) positive ion: 506.1422 m/z, $[M]^+$ (calc. 506.1422). Data for **1b**: **$^1$H NMR** (500 MHz, $CD_2Cl_2$): δ 8.05 (t, $^3J_{HH}$ = 8.2, 1H, py), 7.70 – 7.75 (m, 8H, $Ar^F$), 7.56 (br, 4H, $Ar^F$), 7.49 (d, $^3J_{HH}$ = 2.3, 2H, imid), 7.18 (d, $^3J_{HH}$ = 8.2, 2H, py), 7.12 (d, $^3J_{HH}$ = 2.3, 2H, imid), 4.17 (t, $^3J_{HH}$ = 6.5, 4H, *N*-$CH_2$), 1.91 (app. p, *J* = 6, 4H, $CH_2$), 1.24 – 1.48 (m, 16H, $CH_2$). **$^{13}$C{$^1$H} NMR** (101 MHz, $CD_2Cl_2$): δ 196.8 (d, $^1J_{RhC}$ = 78, carbonyl), 186.5 (d, $^1J_{RhC}$ = 48, carbene), 162.3 (q, $^1J_{CB}$ = 50, $Ar^F$), 152.7 (s, py), 146.3 (s, py), 135.4 (s, $Ar^F$), 129.5 (q, $^2J_{FC}$ = 32, $Ar^F$), 125.2 (q, $^1J_{FC}$ = 272, $Ar^F$), 123.2 (s, imid), 118.1 (sept, $^3J_{FC}$ = 4, $Ar^F$), 117.5 (s, imid), 106.7 (s, py), 51.7 (s, *N*-$\underline{C}H_2CH_2$), 30.6 (s, $CH_2$), 29.0 (s, $CH_2$), 28.8 (s, $CH_2$), 28.5 (s, $CH_2$), 25.4 (s, $CH_2$). **ESI-MS** ($CH_3CN$, 180 °C, 3 kV): positive ion: 508.1570 *m/z*, $[M]^+$ (calc. 508.1578). **Anal**. Calcd for $C_{56}H_{43}BF_{24}N_5ORh$ (1371.65 g $mol^{-1}$): C, 49.04; H, 3.16; N, 5.11. Found: C, 49.17; H, 3.07; N, 5.10. **IR** ($CH_2Cl_2$): ν(CO) 1986 $cm^{-1}$. **IR** ($CH_3CN$) ν(CO) 1977 $cm^{-1}$.

***[Rh(CNC-$(CH_2)_{12}$)(CO)($CH_3$)I][$BAr^F_4$] (3b)***

To a purple solution of **1b** (0.033 g, 0.024 mmol) in $CH_2Cl_2$ (5 mL), was added MeI (0.0075 mL, 0.120 mmol). The solution was stirred at room temperature for 3 hours and the product precipitated by addition of excess pentane. The product as a cream powder was isolated by filtration, washed with pentane (2x5 mL) and dried in vacuo. Yield: 0.028 g (75%). **$^1$H NMR** (500 MHz, $CD_2Cl_2$): δ 8.34 (t, $^3J_{HH}$ = 8.2, 1H, py), 7.78 (d, $^3J_{HH}$ = 2.2, 2H, imid), 7.70 – 7.74 (m, 8H, $Ar^F$), 7.56 (d, $^3J_{HH}$ = 8.2, 2H, py), 7.55 (br, 4H, $Ar^F$), 7.28 (d, $^3J_{HH}$ = 2.2, 2H, imid), 4.25 (app. t, *J* = 8, 4H, *N*-$CH_2$), 2.39 – 2.50 (m, 2H, *N*-$CH_2C\underline{H}_2$), 1.84 – 1.95 (m, 2H, *N*-$CH_2C\underline{H}_2$), 1.30 – 1.75 (m, 16H, $CH_2$), 0.59 (d, $^2J_{RhH}$ = 2.1, 3H, Rh-$CH_3$). **$^{13}$C{$^1$H} NMR** (151 MHz, $CD_2Cl_2$): δ 189.8 (d, $^1J_{RhC}$ = 61, carbonyl), 180.2 ($^1J_{RhC}$ = 37, carbene), 162.3 (q, $^1J_{CB}$ = 50, $Ar^F$), 150.2 (s, py), 145.7 (s, py), 135.3 (s, $Ar^F$), 129.4 (q, $^2J_{CF}$ = 32, $Ar^F$), 125.1 (q, $^1J_{CF}$ = 272, $Ar^F$), 124.3 (s, imid), 118.2 (s, imid), 118.0 (sept, $^3J_{FC}$ = 4, $Ar^F$), 108.8 (s, py), 53.1 (s, *N*-$CH_2$), 30.1 (s, *N*-$CH_2\underline{C}H_2$), 29.5 (s, $CH_2$), 28.6 (s, $CH_2$), 28.5 (s, $CH_2$), 25.9 (s, $CH_2$), -2.1 (d, $^1J_{RhC}$ = 18, Rh-$CH_3$). **ESI-MS** ($CH_3CN$, 180 °C, 3 kV): positive ion: 650.0849 m/z, $[M]^+$ (calc. 650.0858). **Anal**. Calcd for $C_{57}H_{46}BF_{24}IN_5ORh$ (1513.15 g $mol^{-1}$): C, 45.23; H, 3.06; N, 4.63. Found: C, 45.18; H, 2.97; N, 4.58. **IR** ($CH_2Cl_2$): ν(CO) 2070 $cm^{-1}$. **IR** ($CH_3CN$): ν(CO) 2066 $cm^{-1}$.

***[Rh(CNC-$(CH_2)_{12}$)(CO)$Cl_2$][$BAr^F_4$] (4b)***

A solution of **1b** (0.020 g, 0.015 mmol) and $PhICl_2$ (0.004 g, 0.015 mmol) in $CH_2Cl_2$ (2 mL) was stirred at room temperature for 3 hours. The reaction mixture was layered with pentane and left to stand for 16 hours to give the yellow crystalline product, which was isolated by filtration washed with pentane (2 x 5 mL). Yield: 0.014 g (67%). **$^1$H NMR** (500 MHz, $CD_2Cl_2$): δ 8.43 (t, $^3J_{HH}$ = 8.2, 1H, py), 7.84 (d, $^3J_{HH}$ = 2.2, 2H, imid), 7.70 – 7.75 (m, 8H, $Ar^F$), 7.64 (d, $^3J_{HH}$ = 8.2, 2H, py), 7.56 (s, 4H, $Ar^F$), 7.36 (d, $^3J_{HH}$ = 2.2, 2H, imid), 4.41 (t, $^3J_{HH}$ = 7.7,

4H, *N*-$CH_2$), 2.09 (app. p, *J* = 7, 4H, *N*-$CH_2C\underline{H}_2$), 1.56 (app. p, *J* = 6, 4H, $CH_2$), 1.34 – 1.51 (m, 12H, $CH_2$). **$^{13}C\{^1H\}$ NMR** (101 MHz, $CD_2Cl_2$): δ 181.6 (d, $^1J_{RhC}$ = 57, carbonyl), 173.9 (d, $^1J_{RhC}$ = 33, carbene), 162.3 (q, $^1J_{CB}$ = 49, $Ar^F$), 150.9 (s, py), 147.6 (s, py), 135.4 (s, $Ar^F$), 129.5 (q, $^2J_{CF}$ = 32, $Ar^F$), 125.2 (q, $^1J_{FC}$ = 272, $Ar^F$), 124.7 (s, imid), 119.1 (s, imid), 118.1 (sept, $^3J_{FC}$ = 4, $Ar^F$), 109.9 (s, py), 53.3 (s, *N*-$CH_2$), 31.1 (s, *N*-$CH_2\underline{C}H_2$), 29.2 (s, $CH_2$), 28.6 (s, $CH_2$), 28.1 (s, $CH_2$), 25.6 (s, $CH_2$). **ESI-MS** ($CH_3CN$, 180 °C, 3 kV): positive ion: 578.0958 m/z, $[M]^+$ (calc. 578.0955). **Anal**. Calcd for $C_{56}H_{43}BCl_2F_{24}N_5ORh$ (1442.57 g $mol^{-1}$): C, 46.63; H, 3.00; N, 4.85. Found: C, 46.52; H, 2.85; N, 4.89. **IR** ($CH_2Cl_2$): ν(CO) 2111 $cm^{-1}$.

***[Rh(C^N^C*-$(CH_2)_{12}$)(CO)] (5)***

To a J Young's NMR tube charged with **1a** (0.020 g, 0.014 mmol) and K[$N(SiMe_3)_2$] (0.004 g, 0.020 mmol) was added $C_6D_6$ (0.5 mL) under an argon atmosphere. This resulted in the formation of a red solution and brown precipitate. Quantitative formation of **5** was observed by $^1$H NMR spectroscopy alongside $HN(SiMe_3)_2$ ($\delta_{C\underline{H}3}$ = 0.10, $\delta_{N\underline{H}}$ = -0.07). The red solution was separated by decantation and layered with pentane (under argon). Diffusion of the solvent over 4 hours afforded dark red crystals, which were isolated by decantation, washed with pentane and dried. Yield: 0.003 g (52%). The extremely high reactivity of **5** has prevented accurate elemental analysis results being obtained (on two separate sample batches). Complex **5** is best characterised directly in situ by NMR spectroscopy (see Figures S25–27 for $^1$H and $^{13}C\{^1H\}$ NMR spectra). **$^1$H NMR** (500 MHz, $C_6D_6$, 280 K): δ 6.61 (app. t, *J* = 1, 1H, imid), 6.37 (ddd, $^3J_{HH}$ = 9.1, 5.9, *J* = 1, 1H, py), 6.30 (app. t, *J* = 1, 1H, imid), 6.23 (d app. t, $^3J_{HH}$ = 9.1, *J* = 1, 1H, py), 6.15 (app. t, *J* = 1, 1H, imid), 5.99 (app. t, *J* = 1, 1H, imid), 5.81 (bd, *J* = 1, 1H, py$C\underline{H}$), 5.36 (d app. t, $^3J_{HH}$ = 5.8, *J* = 1, 1H, py), 4.60 (app. t, *J* = 13, 1H, *N*-$C\underline{H}_2CH_2$), 4.58 (d, $^2J_{HH}$ = 13, 1H, py$C\underline{H}_2$), 4.25 (app. t, *J* = 13, 1H, *N*-$C\underline{H}_2CH_2$), 3.72 (d, $^2J_{HH}$ = 12.8, 1H, py$C\underline{H}_2$), 3.32 – 3.40 (m, 1H, *N*-$C\underline{H}_2CH_2$), 3.08 – 3.22 (m, 1H, *N*-$C\underline{H}_2CH_2$), 1.94 – 2.07 (m, 1H, $CH_2$), 1.72 – 1.83 (m, 1H, $CH_2$), 1.03 – 1.63 (m, 18H, $CH_2$).**$^1$H NMR** (500 MHz, $C_6D_6$): δ 6.63 (app. t, *J* = 1, 1H, imid), 6.35 (dd, $^3J_{HH}$ = 9.1, 5.9, 1H, py), 6.33 (app. t, *J* = 1, 1H, imid), 6.20 (d, $^3J_{HH}$ = 9.0, 1H, py), 6.19 (app. t, *J* = 2, 1H, imid), 6.04 (app. t, *J* = 1, 1H, imid), 5.79 (br, 1H, py$C\underline{H}$), 5.35 (d, $^3J_{HH}$ = 5.8, 1H, py), 4.58 (app. br, 2H, py$C\underline{H}_2$ + *N*-$C\underline{H}_2CH_2$), 4.23 (s, 1H, *N*-$C\underline{H}_2CH_2$), 3.76 (bs, 1H, py$C\underline{H}_2$), 3.41 (br, 1H, *N*-$C\underline{H}_2CH_2$), 3.22 (br, 1H, *N*-$C\underline{H}_2CH_2$), 1.99 (br, 1H, $CH_2$), 1.75 (br, 1H, $CH_2$), 1.00 - 1.66 (m, 18H, $CH_2$). **$^{13}C\{^1H\}$ NMR** (101 MHz, $C_6D_6$): δ 197.4 (d, $^1J_{RhC}$ = 73, carbonyl) 185.5 (d, $^1J_{RhC}$ = 43, carbene), 174.2 (d, $^1J_{RhC}$ = 44, carbene), 149.5 (s, py), 143.2 (s, py), 126.6 (s, py), 119.7 (s, py), 119.5 (s, imid), 119.3 (s, imid), 119.1 (s, imid), 117.7 (s, imid), 100.1 (s, py), 94.4 (s, py$\underline{C}H$), 58.2 (s, py$\underline{C}H_2$), 51.4 (s, *N*-$\underline{C}H_2CH_2$), 50.7 (s, *N*-$\underline{C}H_2CH_2$), 32.1 (s, $CH_2$), 31.0 (s, $CH_2$), 28.0 (s, $CH_2$), 27.8 (s, $CH_2$), 27.7 (s, $CH_2$), 27.6 (s, $CH_2$), 26.5 (s, $CH_2$), 24.8 (s, $CH_2$), 24.0 (s, $CH_2$). **IR** ($C_6H_6$): ν(CO): 1929 $cm^{-1}$.

**In situ NMR experiments**

***Preparation of [Rh(C^N^C-$(CH_2)_{12}$)(CO)($CH_3$)I][$BAr^F_4$] (3a)***

To a solution of **1a** (0.008 g, 0.006 mmol) in $CD_2Cl_2$ (0.5 mL) inside a J Young's NMR tube was added MeI (0.018 mL, 0.285 mmol) under an argon atmosphere. The J. Young's NMR tube was sealed and monitored

periodically by $^{1}$H NMR spectroscopy. After 3 hours, less than 5% **1a** was present. The reaction tube was left to stand for a further 17 hours, after which no signals of **1a** were observable. The product **3a** was characterised in situ by NMR spectroscopy. ESI-MS and IR data were obtained from crude (impure) mixtures of **3a** prepared in a similar manner, with excess MeI removed in vacuo. **$^{1}$H NMR** (500 MHz, $CD_2Cl_2$): δ 8.04 (t, $^{3}J_{HH}$ = 7.8, 1H, py), 7.70 – 7.75 (m, 8H, $Ar^F$), 7.63 (d, $^{3}J_{HH}$ = 7.8, 2H, py), 7.55 (br, 4H, $Ar^F$), 7.26 (d, $^{3}J_{HH}$ = 1.7, 2H, imid), 7.19 (d, $^{3}J_{HH}$ = 1.7, 2H, imid), 5.4 (br, 2H, py$C\underline{H}_2$), 5.1 (vbr, 2H, *N*-$C\underline{H}_2CH_2$), 4.1 (br, 2H, *N*-$C\underline{H}_2CH_2$), 1.76 – 2.05 (br m, 4H, $CH_2$), 1.23 – 1.55 (m, $CH_2$, 16H), 1.20 (d, $^{2}J_{RhH}$ = 1.8, Rh-Me); one py$C\underline{H}_2$ resonance (2H) was too broad to definitively locate at this temperature. **$^{13}$C{$^{1}$H} NMR** (126 MHz, $CD_2Cl_2$, selected data only): δ 189.4 (d, $^{1}J_{RhC}$ = 64, carbonyl), 165.1 (d, $^{1}J_{RhC}$ = 34, carbene), -1.2 (d, $^{2}J_{RhH}$ = 20, Rh-$CH_3$). **ESI-MS** ($CH_3CN$, 180 °C, 3 kV) positive ion: 678.1169 m/z, $[M]^+$ (calc. 678.1171). **IR** ($CH_2Cl_2$): ν(CO) 2067 $cm^{-1}$.

***Preparation of [Rh(C^N^C-$(CH_2)_{12}$)(CO)$Cl_2$][$BAr^F_4$] (4a)***

To a J Young's NMR tube charged with **1a** (0.008 g, 0.006 mmol) and $PhICl_2$ (0.002 g, 0.007 mmol) was added $CD_2Cl_2$ (0.5 mL) under an argon atmosphere. This resulted in a rapid colour change from yellow to pale yellow and quantitative formation of **4a**, which was characterised immediately in situ by NMR spectroscopy. ESI-MS and IR data were obtained from crude (impure) mixtures of **4a** prepared in a similar manner and passed through a silica plug. **$^{1}$H NMR** (500 MHz, $CD_2Cl_2$): δ 8.09 (t, $^{3}J_{HH}$ = 7.7, 1H, py), 7.70 – 7.75 (m, 8H, $Ar^F$), 7.68 (d, $^{3}J_{HH}$ = 7.8, 2H, py), 7.56 (br, 4H, $Ar^F$), 7.34 (d, $^{3}J_{HH}$ = 1.6, 2H, imid), 7.26 (d, $^{3}J_{HH}$ = 1.8, 2H, imid), 6.63 (d, $^{2}J_{HH}$ = 15.8, 2H, py$C\underline{H}_2$), 5.21 (d, $^{2}J_{HH}$ = 15.8, 2H, py$C\underline{H}_2$), 4.65 (ddd, $^{2}J_{HH}$ = 14.7, $^{3}J_{HH}$ = 12.8, 4.2, 2H, *N*-$CH_2$), 4.12 (ddd, $^{2}J_{HH}$ = 14.7, $^{3}J_{HH}$ = 12.5, 5.7, 2H, *N*-$C\underline{H}_2CH_2$), 1.98 – 2.11 (m, 2H, $CH_2$), 1.86 – 1.98 (m, 2H, $CH_2$), 1.38 – 1.61 (m, 10H, $CH_2$), 1.12 – 1.36 (m, 6H, $CH_2$). **$^{13}$C{$^{1}$H} NMR** (126 MHz, $CD_2Cl_2$, selected data only): δ 180.7 (d, $^{1}J_{RhC}$ = 57, carbonyl), 160.1 (d, $^{1}J_{RhC}$ = 30, carbene). **ESI-MS** ($CH_3CN$, 180 °C, 3 kV) positive ion: 606.1271 m/z, $[M]^+$ (calc. 606.1268). **IR** ($CH_2Cl_2$): ν(CO) 2110 $cm^{-1}$.

**X-ray crystallography**

Crystallographic data for **1a**, **1a***, **1b**, **3b**, **4b** and **5** are summarised in Table 2. Data were collected on an Oxford Diffraction Gemini Ruby CCD diffractometer using graphite monochromated Mo Kα (*λ* = 0.71073 Å) or CuKα (λ = 1.54178 Å) radiation and a low-temperature device [150(2) K]. Data were collected and reduced using CrysAlisPro.[38] All non-hydrogen atoms were refined anisotropically using SHELXL,[39] through the Olex2 interface.[40] Hydrogen atoms were placed in calculated positions using the riding model. Full crystallographic details are documented in CIF format and have been deposited with the Cambridge Crystallographic Data Centre (see Table 2). These data can be obtained free of charge via www.ccdc.cam.ac.uk/data_request/cif.

**Table 2:** Crystallographic data.

| | **1a** | **1a*** | **1b** | **3b** | **4b**·$^1/_2CH_2Cl_2$ | **5**·$^1/_3C_6H_6$ |
|---|---|---|---|---|---|---|
| CCDC | 1025594 | 1027503 | 1025595 | 1025596 | 1025597 | 1025598 |
| Formula | $C_{58}H_{47}BF_{24}N_5ORh$ | $C_{58}H_{47}BF_{24}N_5ORh$ | $C_{56}H_{43}BF_{24}N_5ORh$ | $C_{57}H_{46}BF_{24}IN_5ORh$ | $C_{56.5}H_{44}BCl_3F_{24}N_5ORh$ | $C_{28}H_{36}N_5ORh$ |
| *M* | 1399.72 | 1399.72 | 1371.67 | 1513.61 | 1485.03 | 561.53 |
| Crystal System | Triclinic | Triclinic | Monoclinic | Monoclinic | Triclinic | Trigonal |
| Space group | *P*-1 | *P*-1 | $P2_1/c$ | $P2_1/c$ | *P*-1 | *R*-3 |
| Radiation | MoKα | CuKα | MoKα | MoKα | MoKα | MoKα |
| *a* [Å] | 9.3661(3) | 13.0450(10) | 13.3809(5) | 14.26866(15) | 12.7330(4) | 19.2242(2) |
| *b* [Å] | 18.7809(6) | 14.5880(14) | 28.7207(11) | 17.1057(2) | 15.5875(4) | 19.2242(2) |
| *c* [Å] | 19.3860(6) | 17.4059(11) | 16.9649(7) | 24.6768(3) | 17.0556(5) | 37.5121(8) |
| *a* [deg] | 116.409(3) | 104.723(7) | 90 | 90 | 100.337(2) | 90 |
| $\beta$ [deg] | 94.878(3) | 105.186(7) | 105.369(4) | 94.4576(10) | 97.165(2) | 90 |
| *g* [deg] | 92.986(3) | 102.973(8) | 90 | 90 | 113.343(3) | 120 |
| *V* [Å$^3$] | 3027.66(18) | 2937.5(4) | 6286.6(5) | 6004.79(12) | 2984.89(16) | 12006.0(4) |
| *Z* | 2 | 2 | 4 | 4 | 2 | 18 |
| Density [gcm$^{-3}$] | 1.535 | 1.582 | 1.449 | 1.674 | 1.652 | 1.398 |
| $\mu$ (mm$^{-1}$) | 0.400 | 3.452 | 0.384 | 0.918 | 0.541 | 0.669 |
| $\theta$ range [deg] | $3.16 \le \theta \le 26.37°$ | $6.49 \le \theta \le 66.58°$ | $3.32 \le \theta \le 26.37°$ | $3.10 \le \theta \le 26.37°$ | $2.94 \le \theta \le 26.37°$ | $2.98 \le \theta \le 26.37°$ |
| Reflns collected | 23522 | 18880 | 96566 | 70014 | 29569 | 89168 |
| $R_{int}$ | 0.0340 | 0.1078 | 0.0638 | 0.0348 | 0.0287 | 0.0444 |
| Completeness | 99.8% | 99.8% | 99.8% | 99.8% | 99.8% | 99.8% |
| No. of data/restr/ param | 12359/852/960 | 10378/830/924 | 12828/1087/955 | 12268/885/909 | 12186/373/852 | 5442/459/389 |
| $R_1$ [$I > 2\sigma(I)$] | 0.0495 | 0.0803 | 0.0546 | 0.0446 | 0.0474 | 0.0374 |
| $wR_2$ [all data] | 0.1117 | 0.2151 | 0.1572 | 0.1141 | 0.1184 | 0.0958 |
| *GoF* | 1.051 | 1.018 | 1.040 | 1.053 | 1.037 | 1.078 |
| Largest diff. pk and hole [eÅ$^{-3}$] | 0.69/-0.53 | 0.89/-1.10 | 0.94/-0.59 | 2.62/-0.96 | 1.05/-0.92 | 1.75/-0.22 |

**Supporting information**

X-ray crystallographic data for complexes **1a**, **1a***, **1b**, **3b**, **4b** and **5** in CIF format. Selected NMR and UV-vis absorption spectra. This material is available free of charge via the Internet at http://pubs.acs.org.

**Acknowledgements**

We thank the University of Warwick (R.E.A.) and the Royal Society (A.B.C.) for financial support. Crystallographic data was collected using a diffractometer purchased through support from Advantage West Midlands and the European Regional Development Fund.

**References**

1 (a) van Koten, G., Milstein, D. Eds.; *Top. Organomet. Chem.* **2013**, *40*, 1-352; (b) Albrecht, M.; Lindner, M. M. *Dalton Trans.* **2011**, *40*, 8733–8744; (c) van der Boom, M. E.; Milstein, D. *Chem. Rev.* **2003**, *103*, 1759–1792; (d) Albrecht, M.; van Koten, G. *Angew. Chem. Int. Ed.* **2001**, *40*, 3750–3781.

2 (a) Yao, W.; Zhang, Y.; Jia, X.; Huang, Z. *Angew. Chem. Int. Ed.* **2014**, *53*, 1390–1394; (b) Haibach, M. C.; Kundu, S.; Brookhart, M.; Goldman, A. S. *Acc. Chem. Res.* **2012**, *45*, 947–958; (c) Choi, J.; MacArthur, A. H. R.; Brookhart, M.; Goldman, A. S. *Chem. Rev.* **2011**, *111*, 1761–1779.

3 (a) Feller, M.; Diskin-Posner, Y.; Shimon, L. J. W.; Ben-Ari, E.; Milstein, D. *Organometallics* **2012**, *31*, 4083–4101; (b) Schwartsburd, L.; Iron, M. A.; Konstantinovski, L.; Ben-Ari, E.; Milstein, D. *Organometallics* **2011**, *30*, 2721–2729.

4 Selected examples: (a) Chang, Y.-H.; Nakajima, Y.; Tanaka, H.; Yoshizawa, K.; Ozawa, F. *J. Am. Chem. Soc.* **2013**, *135*, 11791–11794; (b) Filonenko, G. A.; Conley, M. P.; Copéret, C.; Lutz, M.; Hensen, E. J. M.; Pidko, E. A. *ACS Catal.* **2013**, *3*, 2522–2526 (c) van der Vlugt, J. I.; Pidko, E. A.; Bauer, R. C.; Gloaguen, Y.; Rong, M. K.; Lutz, M. *Chem. Eur. J.* **2011**, *17*, 3850–3854; (d) Gunanathan, C.; Milstein, D. *Acc. Chem. Res.* **2011**, *44*, 588–602; (e) Balaraman, E.; Gnanaprakasam, B.; Shimon, L. J. W.; Milstein, D. *J. Am. Chem. Soc.* **2010**, *132*, 16756–16758; (f) van der Vlugt, J. I.; Siegler, M. A.; Janssen, M.; Vogt, D.; Spek, A. L. *Organometallics* **2009**, *28*, 7025–7032. (g) van der Vlugt, J. I.; Reek, J. N. H. *Angew. Chem. Int. Ed.* **2009**, *48*, 8832–8846; (h) Kohl, S. W.; Weiner, L.; Schwartsburd, L.; Konstantinovski, L.; Shimon, L. J. W.; Ben-David, Y.; Iron, M. A.; Milstein, D. *Science* **2009**, *324*, 74–77; (i) Tanaka, R.; Yamashita, M.; Nozaki, K. *J. Am. Chem. Soc.* **2009**, *131*, 14168–14169; (j) Gunanathan, C.; Ben-David, Y.; Milstein, D. *Science* **2007**, *317*, 790–792.

5 (a) Filonenko, G. A.; Cosimi, E.; Lefort, L.; Conley, M. P.; Copéret, C.; Lutz, M.; Hensen, E. J. M.; Pidko, E. A. *ACS Catal.* **2014**, *4*, 2667–2671; (b) Hernández-Juárez, M.; Vaquero, M.; Álvarez, E.; Salazar, V.; Suárez, A. *Dalton Trans.* **2013**, *42*, 351–354; (c) Sun, Y.; Koehler, C.; Tan, R.; Annibale, V. T.; Song, D. *Chem. Commun.* **2011**, *47*, 8349–8351.

[6] Reviews: (a) Poyatos, M.; Mata, J. A.; Peris, E. *Chem. Rev.* **2009**, *109*, 3677–3707; (b) Pugh, D.; Danopoulos, A. A. *Coord. Chem. Rev.* **2007**, *251*, 610–641; (c) Peris, E.; Crabtree, R. H. *Coord. Chem. Rev.* **2004**, *248*, 2239–2246. Other selected examples: (d) Serra, D.; Cao, P.; Cabrera, J.; Padilla, R.; Rominger, F.; Limbach, M. *Organometallics* **2011**, *30*, 1885–1895; (e) Schultz, K. M.; Goldberg, K. I.; Gusev, D. G.; Heinekey, D. M. *Organometallics* **2011**, *30*, 1429–1437; (f) Inamoto, K.; Kuroda, J.-I.; Kwon, E.; Hiroya, K.; Doi, T. *J. Organomet. Chem.* **2009**, *694*, 389–396; (g) Wei, W.; Qin, Y.; Luo, M.; Xia, P.; Wong, M. S. *Organometallics* **2008**, *27*, 2268–2272. (h) Danopoulos, A. A.; Pugh, D.; Wright, J. A. *Angew. Chem. Int. Ed.* **2008**, *47*, 9765–9767; (i) Danopoulos, A. A.; Wright, J. A.; Motherwell, W. B.; Ellwood, S. *Organometallics* **2004**, *23*, 4807–4810. (j) Douthwaite, R. E.; Houghton, J.; Kariuki, B. M. *Chem. Commun.* **2004**, 698–699.

[7] Representative examples: (a) Hahn, F. E.; Jahnke, M. C.; Pape, T. *Organometallics* **2007**, *26*, 150–154; (b) Hahn, F. E.; Jahnke, M. C.; Gomez-Benitez, V.; Morales-Morales, D.; Pape, T. *Organometallics* **2005**, *24*, 6458–6463; (c) Nielsen, D. J.; Cavell, K. J.; Skelton, B. W.; White, A. H. *Inorg. Chim. Acta* **2002**, *327*, 116–125; (d) Gründemann, S.; Albrecht, M.; Loch, J. A.; Faller, J. W.; Crabtree, R. H. *Organometallics* **2001**, *20*, 5485–5488 (e) Peris, E.; Mata, J.; Loch, J. A.; Crabtree, R. H. *Chem. Commun.* **2001**, 201–202.

[8] (a) Chianese, A. R.; Drance, M. J.; Jensen, K. H.; McCollom, S. P.; Yusufova, N.; Shaner, S. E.; Shopov, D. Y.; Tendler, J. A. *Organometallics* **2014**, *33*, 457–464; (b) Chianese, A. R.; Shaner, S. E.; Tendler, J. A.; Pudalov, D. M.; Shopov, D. Y.; Kim, D.; Rogers, S. L.; Mo, A. *Organometallics* **2012**, *31*, 7359–7367; (c) Chianese, A. R.; Mo, A.; Lampland, N. L.; Swartz, R. L.; Bremer, P. T. *Organometallics* **2010**, *29*, 3019–3026.

[9] (a) Meyer, K.; Dalebrook, A. F.; Wright, L. J. *Dalton Trans.* **2012**, *41*, 14059–14067; (b) Saito, S.; Azumaya, I.; Watarai, N.; Kawasaki, H.; Yamasaki, R. *Heterocycles* **2009**, *79*, 531–548.

[10] Crowley, J. D.; Goldup, S. M.; Lee, A.-L.; Leigh, D. A.; McBurney, R. T. *Chem. Soc. Rev.* **2009**, *38*, 1530.

[11] Andrew, R. E.; Chaplin, A. B. *Dalton Trans.* **2014**, *43*, 1413–1423.

[12] (a) Frey, G. D.; Rentzsch, C. F.; Preysing, von, D.; Scherg, T.; Mühlhofer, M.; Herdtweck, E.; Herrmann, W. A. *J. Organomet. Chem.* **2006**, *691*, 5725–5738; (b) Poyatos, M.; Uriz, P.; Mata, J. A.; Claver, C.; Fernandez, E.; Peris, E. *Organometallics* **2003**, *22*, 440–444.

[13] Wilson, J. M.; Sunley, G. J.; Adams, H.; Haynes, A. *J. Organomet. Chem.* **2005**, *690*, 6089–6095.

[14] Wright, J. A.; Danopoulos, A. A.; Motherwell, W. B.; Carroll, R. J.; Ellwood, S.; Saßmannshausen, J. *Chem. Ber.* **2006**, *2006*, 4857–4865.

[15] Simons, R. S.; Custer, P.; Tessier, C. A.; Youngs, W. J. *Organometallics* **2003**, *22*, 1979–1982.

[16] (a) Wucher, B.; Moser, M.; Schumacher, S. A.; Rominger, F.; Kunz, D. *Angew. Chem. Int. Ed.* **2009**, *48*, 4417–4421; (b) Moser, M.; Wucher, B.; Kunz, D.; Rominger, F. *Organometallics* **2007**, *26*, 1024–1030.

[17] See for example: (a) Nielsen, D. J.; Cavell, K. J.; Skelton, B. W.; White, A. H. *Inorg. Chim. Acta* **2006**, *359*, 1855–1869; (b) Loch, J. A.; Albrecht, M.; Peris, E.; Mata, J.; Faller, J. W.; Crabtree, R. H. *Organometallics* **2002**, *21*, 700–706.

[18] See for example: (a) Nawara-Hultzsch, A. J.; Stollenz, M.; Barbasiewicz, M.; Szafert, S.; Lis, T.; Hampel, F.; Bhuvanesh, N.; Gladysz, J. A. *Chem. Eur. J.* **2014**, *20*, 4617–4637; (b) Zeits, P. D.; Rachiero, G. P.; Hampel, F.; Reibenspies, J. H.; Gladysz, J. A. *Organometallics* **2012**, *31*, 2854–2877; (c) Ayme, J.-F.; Lux, J.; Sauvage, J.-P.; Sour, A. *Chem. Eur. J.* **2012**, *18*, 5565–5573; (d) Goldup, S. M.; Leigh, D. A.; Lusby, P. J.; McBurney, R. T.; Slawin, A. M. Z. *Angew. Chem. Int. Ed.* **2008**, *47*, 6999–7003; (e) Nawara, A.; Shima, T.; Hampel, F.; Gladysz, J. *J. Am. Chem. Soc.* **2006**, *128*, 4962–4963; (f) Fuller, A.-M. L.; Leigh, D. A.; Lusby, P. J.; Slawin, A. M. Z.; Walker, D. B. *J. Am. Chem. Soc.* **2005**, *127*, 12612–12619 (g) Chambron, J.-C.; Collin, J.-P.; Heitz, V.; Jouvenot, D.; Kern, J.-M.; Mobian, P.; Pomeranc, D.; Sauvage, J.-P. *Eur. J. Org. Chem.* **2004**, *2004*, 1627–1638.

[19] (a) Wang, L.; Hampel, F.; Gladysz, J. A. *Angew. Chem. Int. Ed.* **2006**, *45*, 4372–4375; (b) Wang, L.; Shima, T.; Hampel, F.; Gladysz, J. *Chem. Commun.* **2006**, *2006*, 4075–4077; (c) Bauer, E. B.; Ruwwe, J.; Hampel, F. A.; Szafert, S.; Gladysz, J. A.; Martín-Alvarez, J. M.; Peters, T. B.; Bohling, J. C.; Lis, T. *Chem. Commun.* **2000**, 2261–2262.

[20] Raba, A.; Anneser, M. R.; Jantke, D.; Cokoja, M.; Herrmann, W. A.; Kühn, F. E. *Tet. Lett.* **2013**, *54*, 3384–3387.

[21] No reaction is observed when placing pure **1b** under $H_2$ (4 atm), implicating the external hydrogenation catalyst in this decomposition/undesired reactivity.

[22] Vazquez-Serrano, L. D.; Owens, B. T.; Buriak, J. M. *Inorg. Chim. Acta* **2006**, *359*, 2786–2797.

[23] Miecznikowski, J. R.; Gründemann, S.; Albrecht, M.; Mégret, C.; Clot, E.; Faller, J. W.; Eisenstein, O.; Crabtree, R. H. *Dalton Trans.* **2003**, 831–838.

[24] We are currently investigating the reaction of **1a** with carbon monoxide. Full details will be reported in due course, however, we do note here that placing **1a** under a carbon monoxide atmosphere induces atropisomerisation, consistent with coordination of carbon monoxide. Similar dynamics has been studied in related palladium NHC systems, which are promoted by coordination of the counter anion.[23] The solution of the symmetrical polymorph **1a** contains a highly disordered solvent molecule (removed using the SQUEEZE algorithm – Spek, A. L. *Acta Cryst.* **2009**, *D65*, 148–155), while no solvent is present in the solution of **1a***: alternatively implicating crystal-packing effects.

[25] Feller, M.; Ben-Ari, E.; Gupta, T.; Shimon, L. J. W.; Leitus, G.; Diskin-Posner, Y.; Weiner, L.; Milstein, D. *Inorg. Chem.* **2007**, *46*, 10479–10490.

[26] (a) Bera, J. K.; Dunbar, K. R. *Angew. Chem. Int. Ed.* **2002**, *41*, 4453–4457; (b) Connick, W. B.; Marsh, R. E.; Schaefer, W. P.; Gray, H. B. *Inorg. Chem.* **1997**, *36*, 913–922; (c) Novoa, J. J.; Aullón, G.; Alemany,

P.; Alvarez, S. *J. Am. Chem. Soc.* **1995**, *117*, 7169–7171; (d) *Extended Linear Chain Compounds, Vol 3.; Miller, J. S.* Ed.; Plenum: New York, 1982; (e) Mann, K. R.; Gordon, J. G.; Gray, H. B. *J. Am. Chem. Soc.* **1975**, *97*, 3553–3555. (f) Krogmann, K. *Angew. Chem. Int. Ed.* **1969**, *8*, 35–42.

[27] Selected rhodium examples: (a) Laurila, E.; Oresmaa, L.; Hassinen, J.; Hirva, P.; Haukka, M. *Dalton Trans.* **2013**, *42*, 395–398; (b) Inoki, D.; Matsumoto, T.; Nakai, H.; Ogo, S. *Organometallics* **2012**, *31*, 2996–3001; (c) Mitsumi, M.; Umebayashi, S.; Ozawa, Y.; Tadokoro, M.; Kawamura, H.; Toriumi, K. *Chem. Lett.* **2004**, *33*, 970–971; (d) Prater, M. E.; Pence, L. E.; Clérac, R.; Finniss, G. M.; Campana, C.; Auban-Senzier, P.; Jérome, D.; Canadell, E.; Dunbar, K. R. *J. Am. Chem. Soc.* **1999**, *121*, 8005–8016.

[28] (a) Helps, I. M.; Matthes, K. E.; Parker, D.; Ferguson, G. *J. Chem. Soc., Dalton Trans.* **1989**, 915–920. (b) Ferguson, G.; Matthes, K. E.; Parker, D. *J. Chem. Soc., Chem. Commun.* **1987**, 1350–1351.

[29] (a) Tran, N. T.; Stork, J. R.; Pham, D.; Olmstead, M. M.; Fettinger, J. C.; Balch, A. L. *Chem. Commun.* **2006**, 1130; (b) Mann, K. R.; Thich, J. A.; Bell, R. A.; Coyle, C. L.; Gray, H. B. *Inorg. Chem.* **1980**, *19*, 2462–2468; (c) Mann, K. R.; Lewis, N. S.; Williams, R. M.; Gray, H. B.; Gordon, J. G. *Inorg. Chem.* **1978**, *17*, 828–834.

[30] Rice, S. F.; Gray, H. B. *J. Am. Chem. Soc.* **1981**, *103*, 1593–1595.

[31] Hartwig, J. F., *Organotransition Metal Chemistry*; University Science Books: Mil Valley, 2010.

[32] Taylor, R. T.; Stevenson, T. A. *Tet. Lett.* **1988**, *29*, 2033–2036.

[33] Feller, M.; Diskin-Posner, Y.; Leitus, G.; Shimon, L. J. W.; Milstein, D. *J. Am. Chem. Soc.* **2013**, *135*, 11040–11047.

[34] Schaub, T.; Radius, U.; Diskin-Posner, Y.; Leitus, G.; Shimon, L. J. W.; Milstein, D. *Organometallics* **2008**, *27*, 1892–1901.

[35] (a) Gloaguen, Y.; Rebreyend, C.; Lutz, M.; Kumar, P.; Huber, M.; van der Vlugt, J. I.; Schneider, S.; de Bruin, B. *Angew. Chem. Int. Ed.* **2014**, *53*, 6814–6818; (b) Khaskin, E.; Diskin-Posner, Y.; Weiner, L.; Leitus, G.; Milstein, D. *Chem. Commun.* **2013**, *49*, 2771–2773. (c) Schwartsburd, L.; Iron, M. A.; Konstantinovski, L.; Diskin-Posner, Y.; Leitus, G.; Shimon, L. J. W.; Milstein, D. *Organometallics* **2010**, *29*, 3817–3827. (d) Ben-Ari, E.; Leitus, G.; Shimon, L. J. W.; Milstein, D. *J. Am. Chem. Soc.* **2006**, *128*, 15390–15391.

[36] Buschmann, W. E.; Miller, J. S.; Bowman-James, K.; Miller, C. N. *Inorg. Synth.* **2002**, *33*, 83–91.

[37] McCleverty, J. A.; Wilkinson, G.; Lipson, L. G.; Maddox, M. L.; Kaesz, H. D. *Inorg. Synth.* **1990**, *28*, 84–86.

[38] Oxford Diffraction Ltd, Abingdon, England: 2014.

[39] Sheldrick, G. M. *Acta Cryst.* **2008**, *A64*, 112–122.

[40] Dolomanov, O. V.; Bourhis, L. J.; Gildea, R. J; Howard, J. A. K.; Puschmann, H. *J. Appl. Cryst.* **2009**, *42*, 339–341.

## TOC graphic

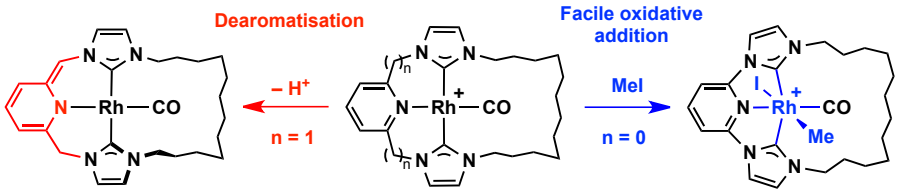


Synthesis using metal-template promoted ring closing olefin metathesis

## Synopsis

Macrocyclic rhodium carbonyl complexes containing tridentate CNC macrocycles with dodecamethylene spacers have been prepared using metal-template promoted ring closing olefin metathesis. Systems containing both lutidine and pyridine based CNC backbones have been synthesised and their dynamics and reactivity comparatively investigated.